Charging Optimization for Li-ion Battery in Electric Vehicles: A Review

Cuili Chen, *Member, IEEE*, Zhongbao Wei, *Senior Member, IEEE*, and Alois Christian Knoll, *Senior Member, IEEE*

***Abstract*—Battery Electric Vehicles (BEVs) are advocated due to their environmental benign characteristic. However, the long charging time and the degradation caused by fast charging impedes their further popularization. Extensive research has been carried out to optimize the charging process, such as minimizing charging time and aging, of Lithium-ion Batteries (LIBs). Motivated by this, a comprehensive review of existing Charging Optimization (ChgOp) techniques is provided in this paper. Firstly, the operation and models for LIBs are explained. Then, unexpected side effects especially for the aging mechanism of LIB associated with unregulated fast charging are scrutinized. This provides a solid theoretical foundation and forms the optimization problem. Following this endeavor, the general framework with critical concerns for ChgOp system design is overviewed. Within this horizon, the state-of-the-art ChgOp techniques, clustered into open- and close-loop categories, are reviewed systematically with their respective merits and shortcomings discussed. Finally, the development of an emerging charging control protocol with both real-time affordability and degradation consciousness is further discussed as an open outlook.**

***Index Terms*— Electric vehicles, Li-ion batteries, charging optimization, battery models, aging mechanism**

I. Introduction

Electric Vehicles (EVs), powered by electric motors, are green mobility tools that mitigate greenhouse gas emissions [1-3]. According to the power source for engines, EVs can be divided into four categories, Battery Electric Vehicles (BEVs), hybrid electric vehicles, plug-in hybrid electric vehicles, and fuel cell electric vehicles. Amongst others, the BEVs have viewed prosperous development due to the high maturity of techniques in addition to the zero-emission capability. The rechargeable battery is one of the vital components of BEVs. In particular, Lithium-ion batteries (LIBs) dominate with 49% market share, followed by lead-acid (43%), NiMH (4%), and NiCd (3%) [4]. LIBs are preferred due to their high specific energy, high specific power, low self-discharge rate, and plunge in costs [5, 6]. However, LIBs also have some limitations which hamper the broad application of BEVs. One of them is the long charging time.

Battery charging has been a vast field of investigation over years [7]. Nowadays, LIBs are generally charged with a Constant Current-Constant Voltage (CC-CV) or Constant Power-Constant Voltage (CP-CV) approach. In general, the recommended charging rate of LIBs is 0.5C - 1C [8]. For instance, battery manufacturers recommend a charging rate equal to or less than 0.8C to prolong battery lifespan [8, 9]. Consequently, it will take several hours for the battery to be fully charged [10, 11]. During these charging processes, more than 60% of the time is spent on the CV phase. For example, for the SE US18650FT Sony cell with a nominal capacity of 1.1Ah, the recommended charging current is 1.05A, suggesting that fully charging the battery takes more than 2.5h [12]. The time can be longer when it comes to battery packs due to the equalization process [13]. The slow charging of LIBs is one of the major limitations for the vast acceptance of BEVs. With the 'range anxiety', the increment of pack capacity is imperative. This means a further elongated charging time [14] which exacerbates the situation.

To address the issue, fast-charging stations are established. The definition of a fast-charging station varies [15-17]. In this paper, charging stations capable of delivering more than 50 kW are treated as fast-charging stations. In general, the capacities of the battery packs in BEVs are between 30 kWh and 100 kWh [18]. With fast charging techniques, the time to fully charge the BEV battery packs can be reduced to less than two hours [15]. However, consumers expect BEVs to be charged with enough mileage in 10 to 20 minutes [14, 19], or ideally, the time it takes is comparable to refilling gasoline or diesel vehicles [20] which

Manuscript received 30 August; revised 15 November; accepted 9 December (Corresponding author: Zhongbao Wei). This work was funded by the German Ministry of Education and Research (Bundesministerium für Forschung und Bildung, BMBF) within the NOVBATCON project (reference no. 16EMO0319), which is gratefully acknowledged. Our gratitude also goes to colleagues from VDI/VDE Innovation+Technik GmbH and other colleagues in the NOVBATCON project for their support in the project.

Cuili Chen and Alois Christian Knoll are with the Department of Informatics, Technical University of Munich, Germany. (e-mail: cuili.chen@hotmail.com, knoll@in.tum.de).

Zhongbao Wei is with the National Engineering Laboratory for Electric Vehicles, School of Mechanical Engineering, Beijing Institute of Technology, China. (e-mail: weizb@bit.edu.cn).

is about three minutes [11]. This requirement stimulates the growth of Extreme Fast Charging (XFC) stations [1, 2, 14] and ultra-fast charging stations [21-23], where the charging current is as high as 6C or even above. A comparison of different types of charging stations is summarized in Table I. Slow charging is typically from onboard chargers which are connected to the AC source of the grid and takes 8h to 14h. For semi-fast charging, the socket CCS Combo 2 is used. The BEVs can gain 15 to 50 km per hour charging. Fast charging power rate goes up to 150kW where sockets like CCS Combo 2, Tesla Supercharger, and CHAdeMO**1.1 are used. XFC/ultra-fast charging is generally DC charging with a power rate higher than 350kW. Tesla and Bosch are leading the development in this area [24].

However, fast charging leads to accelerated aging or even safety hazards. Hence, efforts are devoted to optimizing the charging process by balancing different objects, i.e., speeding up the charging, prohibiting the battery aging, and enforcing the physical constraints. Relevant techniques in this area have been reviewed recently. These can be clustered into three categories, namely battery material, charging infrastructure, charging process, and optimization. Authors in [2, 4, 11, 14, 15, 24, 25] discussed the limitations of electrode material and presents the challenges and opportunities for future research. Research regarding the charging infrastructures includes converter topology of the charging station [1, 16, 19, 26, 27], high C-rate charging connectors [28], scheduling model at charging sites [20, 21], economies for charging infrastructure operator [20], the impact of charging stations on the utility grid [3], wireless charging [29, 30]. Research in [24, 31, 32] focuses on the charging process and optimization and summarized some of the charging strategies, authors in [24] especially cover the material and thermal impact on battery charging. Distinguished from such works, this review focuses on the advanced control strategies oriented for LIB's fast Charging Optimization (ChgOp), by including the most recent progress and illustrating the approaches with physical characteristics.

TABLE I COMPARISON OF THE CHARGING STATION FOR BEVS

Charging type	Power rate / kW	Socket type	Charging time	Reference
Slow	<3.7	1 phase AC	8h to 14h (e.g. home charging)	[15, 16]
Semi-fast	3.7 - 50	1 or 3 phase AC, CCS Combo 2*	2h to 8h, 15 to 50 km/h of charging	[3, 16, 19]
Fast	50 - 150	CCS Combo 2, Tesla Supercharger, CHAdeMO**1.1	< 30min, 280 to 300 km/h of charging	[3, 16]
Extreme/ultra-fast	350, 400, 450	Tesla Supercharger, CHAdeMO**1.2	3min to 10min	[22, 24]

* CCS Combo 2: Combined Charging System ** CHAdeMO: CHArge de Move

The remainder of the review is organized as follows. Section II illustrates the fundamentals, namely, structure and operation mechanism, models to simulate the battery operation, and Aging Mechanisms (AMs) associated with fast charging. In section III, the general structure of the ChgOp system is provided, and relevant techniques are clustered into open- and closed-loop techniques accordingly. Corresponding reviews of open-loop and closed-loop ChgOp techniques are presented in Section IV and V, respectively. Conclusions and challenges in fast ChgOp are summarized in Section VI.

II. FUNDAMENTALS OF LIB FOR CHARGING OPTIMIZATION

ChgOp systems are generally developed by following the operation mechanism of LIB to achieve fast charging and/or prohibiting certain AMs. Thus, this section lays the theoretical foundation for the ChgOp system by illustrating the operation mechanism, simulation models, and AMs.

A. Structure and Operation Mechanism of LIB

LIB was developed by Akira Yoshino in 1985 and commercialized by Sony in 1991 [33, 34]. LIB is an electrochemical energy storage system where electrical energy is stored to the bonds of chemicals by synthesizing during charging and the chemical energy is expended during discharging [35]. Fig. 1 shows the typical configuration of a LIB. It includes two current collectors, anode, cathode, and separator socked in lithium salt solution. The anode is expected to have high lithium storage capability and high cycling stability. So far, the most popular anode material is graphite [11, 14, 35-39] which is invented by Rachid Yazami [40]. The cathode material is generally lithium transition-metal oxide which serves as a host of Li-ions so that Li-ions can intercalate/de-intercalate during discharging/charging [14, 35-39]. Popular cathode materials include Lithium Iron Phosphate (LFP), Lithium Cobalt Oxide (LCO), Lithium Nickel Cobalt Aluminum Oxide (NCA), Lithium Nickel Manganese Cobalt Oxide (NMC) [14, 35-39]. The separator is a permeable membrane that allows Li-ions to transfer but is an electronic insulator [36, 41]. In this paper, the charging mechanism is exemplified with the LFP battery which owned the largest share, 36%, in the LIB market [42].

As shown in Fig. 1, in an LFP battery, the negative electrode (anode) is graphite with a layered structure and the positive electrode (cathode) is LFP. LFP has the crystal structure of Olivine in which Li^+ sites in the zigzag octahedral channels formed by FeO_6 and PO_4 [43-45]. Generally, the electrolyte is $LiPF_6$ diluted in Ethylene Carbonate (EC) and Dimethyl Carbonate (DMC), and the separator is polyolefin [41]. The typical thickness of them is shown in Fig. 1 [46].

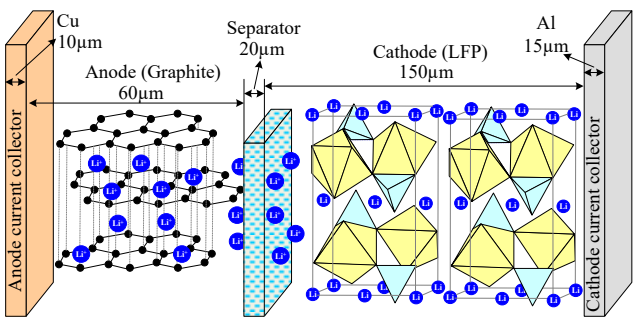

Fig. 1 Structure of a $LiFePO_4$ battery (-) C_n | $LiPF_6$ –EC+DMC | $LiFePO_4$ (+).

When the LFP battery is charging, Li-ions de-intercalates from $LiFePO_4$ and moves from the positive electrode to the

negative electrode, where they intercalated in the layered structure of graphite, vice versa for discharging process. Due to the shuttle of Li-ions between the two electrodes, LIB is also called a rocking-chair battery. The reaction in electrodes can be described as (1).

$$\begin{aligned} &Anode: \quad xLi^+ + xe^- + nC \rightarrow Li_xC_6 \\ &Cathode: \quad LiFePO_4 \rightarrow Li_{1-x}FePO_4 + xLi^+ + xe^- \end{aligned} \tag{1}$$

where normally $0 \leqslant x \leqslant 0.5$ is maintained to be reversibly cyclable [47]. n is the Stoichiometric coefficient of C.

Even though the main reaction stays the same throughout the charging process, the characteristics of LIB varies at different State of Charge (SoC) regime. In general, the charging process can be divided into three phases, Phase I, Phase II, and Phase III, as shown in Fig. 2. Phase I refers to the low SoC regime where the fully discharged battery was charged to 10% of the SoC. Phase II is the medium to high SoC regime until when the battery voltage reaches the predetermined maximum V_{max}. Phase III is the high SoC regime before the predetermined cut-off condition is reached. The charging process can only be optimized when the characteristics are fully perceived. Thus, the following texts give an exhaustive illustration of the characteristics of each phase.

In Phase I, the battery impedance varies dramatically [48-52]. In [51], the LCO battery is investigated. The results show that the battery resistance reduces from about 225mΩ to about 100mΩ. The same characteristics are found in [52] for the NCA battery, where the resistance changes from about 21 mΩ to 17 mΩ. Thus, a low charging rate is recommended [50, 51]. However, an antithetical phenomenon was observed for $LiFePO_4$ batteries in [48], where the internal resistance increases, from 3.5mΩ to about 5mΩ, due to two-phase transition. Thus, a high C-rate is applied at the beginning of charging in [49]. In summary, the charging rate for Phase I should be adjusted according to the cell impedance.

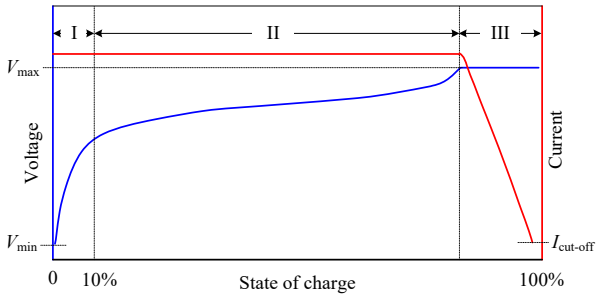

Fig. 2 LIB charging phase.

In Phase II, the battery impedance is stable [48, 51]. A high C-rate charging current can be applied to accelerate the charging process. LIBs' capability of high C-rate charging is influenced by the acceptability of the active materials, cell design, and charging strategy [53]. Authors in [14, 24] discussed the limitation of materials mass transport, battery design and thermal characteristics, and charge transfer perspectives during high C-rate charging. The impacts of porosity and/or tortuosity on concentration polarization are also included. The papers show that improving the electrolyte charge transfer property and reducing the electrode tortuosity helps the battery to achieve a higher charging C-rate. In terms of thermal characteristics, higher temperature accelerate charge transfer but also causes more side reactions and electrode degradations. While, low temperature induces severe lithium deposition. In addition, since the shuttle of Li-ions and lithium deposition also causes battery volume variation, the maximum permissible charging current I_{max} is evaluated by measuring the battery thickness change in [54]. The result shows that the relation between permissible charging current I and the charge quantity x follows the Arrhenius law as $I = a/(x^{0.5})$, a is 4.3, a constant.

In phase III, critical attention is required, because overcharging/overvoltage is liable to happen. In general, the charging current should be well constrained to alleviate the detrimental metallic lithium deposition [51, 52].

B. Battery models

Different models have been developed to simulate the battery behavior, which is critical for the charging strategy design and optimization. This section gives an overview of the predominant models employed in ChgOp research.

1) Electrochemical Model

Electrochemical Models (EcMs) provide insights on the electrochemical process in the battery by following physical principles like Fick's law, Butler-Volmer equation, Nernst equations. Pseudo-two-Dimensional (P2D) model is the most attractive one to researchers. The P2D model is proposed by Prof. Newman's group [55] based on the porous electrode theory. In this theory, the lithium intercalation and de-intercalation process are expressed with several partial differential equations. This P2D model is effective and accurate which has been validated by many studies [56-58]. However, there are more than fifty parameters to be identified which is computationally intensive. In order to reduce the complexity, the Single-Particle Model (SPM) is proposed [59]. SPM treats each electrode as an active particle by assuming that the electrode is very thin and there is no concentration gradient of lithium ions. P2D and SPM are the two EcMs that are frequently adopted in fast ChgOp. For EcM based approaches, additional constraints can be set to restrain AMs. For instance, lithium deposition, a major degradation mechanism, is a cathodic reaction that happens when the over-potential φ is less than 0. Thus, to eliminate the lithium deposition, a constraint is added as shown in (2) [60, 61].

$$\varphi = \Phi_{Electrode} - \Phi_{Electrolyte} - U > 0 \tag{2}$$

where $\Phi_{\text{Electrode}}$ is the potential in the positive and negative electrodes. $\Phi_{\text{Electrolyte}}$ is the potential of the electrolyte. U is the side reaction equilibrium potential and U=0.

During fast charging, the other predominant AM is the side reaction. The side reaction rate can be expressed as (3) [62]. Aging can be deterred by restricting the reaction rate.

This article has been accepted for publication in a future issue of this journal, but has not been fully edited. Content may change prior to final publication. Citation information: DOI 10.1109/TTE.2021.3135525, IEEE Transactions on Transportation Electrification

$$j_{side}^{Li} = -a_{s,side} i_{0,side} e^{(-\frac{a_{s,side} n_{side} F}{RT} \varphi_{side})} \quad (3)$$

where, $a_{s,side}$ is the specific reaction area of the side reaction. $i_{0,side}$ is the exchange current density of the side reaction. $a_{c,side}$ is the cathodic symmetric factor of side reaction. n_{side} is the number of ions involved in the side reaction. F is Faraday constant. R is the universal gas constant. T is the cell temperature in Kelvin. It is worth noting that the lithium deposition and side reaction are two of the most important AMs that have been researched for ChgOp over years.

2) Electrical Equivalent Circuit Model

Electrical Equivalent Circuit Models (ECMs) are applied to emulate electrical performance due to their conciseness and accuracy. A systematical overview of the widely-used ECMs has been given in [63, 64]. Fig. 3 shows four commonly-used ECMs, (a) R_{int} model, (b) n-order RC model, (c) RC equivalent model, and (d) nonlinear double capacitor model. In the R_{int} model, R_{int} consists of the resistance of the electrolyte, the current conductor, and the contact resistance between the electrode and the conductor. There are also nonlinear characteristics during the charging transients which are characterized by RC pairs as shown in Fig. 3(b). The first-order RC model (with only one RC pair) is also known as the Thévenin model in which the RC pair reflects polarization characteristics. The second-order RC model (with two RC pairs) is the most prevalent as it provides a balance between accuracy and complexity. Apart from Fig. 3(a) and Fig. 3(b), the RC equivalent model (Fig. 3(c)) and the nonlinear double capacitor model (Fig. 3(d)) have also been used to assist ChgOp. The ECM has viewed the most widespread applications for LIB state estimation, like the SoC estimation [65-68] and state of power estimation [69]. However, the direct use of them for charging control is not sufficient, since the thermal and degradation behavior, which are critical concerns for charge control, have been overlooked. Table II presents the expressions for the commonly used ECMs.

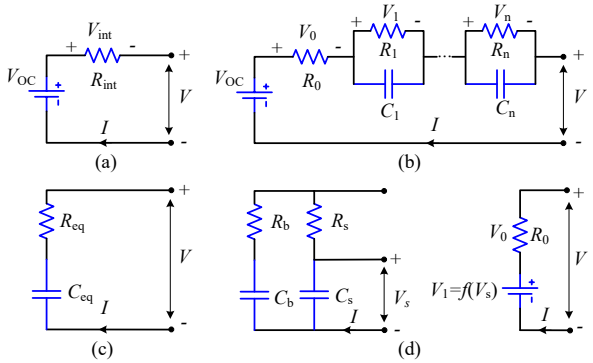

Fig. 3 Battery ECMs. (a) R_{int} model. (b) n-order RC model [70-72]. (c) RC equivalent model [73]. (d) Nonlinear double capacitor model [74]. V_{OC} is the open-circuit voltage. V is the terminal voltage. I is the battery current. R_0, the internal battery resistance, is the same as R_{int}. R_{eq} and C_{eq} are the equivalent resistance and capacitance of the battery. R_S-C_S corresponds to the equivalent resistance and capacitance electrode's surface region; the R_b-C_b represents the equivalent resistance and capacitance of the electrode's bulk inner part.

TABLE II EXPRESSIONS FOR COMMONLY-USED ECMS

Commonly-used ECMs	Expressions
R_{int} model	$\frac{dSOC}{dt} = -\frac{I}{C_{max}}$ $V = V_{OC}(SOC) - I \cdot R_{int}$
n-order RC model	$\frac{dSOC}{dt} = -\frac{I}{C_{max}}$ $\frac{dV_1}{dt} = \frac{I}{C_1} - \frac{V_1}{R_1 C_1}$ … $\frac{dV_n}{dt} = \frac{I}{C_n} - \frac{V_n}{R_n C_n}$ $V = V_{OC}(SOC) - I \cdot R_0 - V_1 - \cdots - V_n$
RC equivalent model [75]	$\frac{dV_{C_{eq}}}{dt} = \frac{I}{C_{eq}}$ $V_{R_{eq}} = I \cdot R_{eq}$ $V = -(V_{C_{eq}} + V_{R_{eq}})$
Nonlinear double capacitor model [74]	$\begin{bmatrix} \dot{V}_b \\ \dot{V}_s \end{bmatrix} = A \begin{bmatrix} V_b \\ V_s \end{bmatrix} + B \cdot I,$ where $A = \begin{bmatrix} -\frac{1}{C_b(R_b+R_s)} & \frac{1}{C_b(R_b+R_s)} \\ \frac{1}{C_s(R_b+R_s)} & -\frac{1}{C_s(R_b+R_s)} \end{bmatrix}$, $B = \begin{bmatrix} \frac{R_s}{C_b(R_b+R_s)} \\ \frac{R_b}{C_s(R_b+R_s)} \end{bmatrix}$ $V = f(V_s) - I \cdot R_0(V_s)$ $f(V_s) = \sum_{i=0}^{5} \alpha_i V_s^i$, where α_i for $i = 0,1,\cdots,5$ are coefficients $R_0(V_s) = \beta_1 + \beta_2 e^{-\beta_3(1-V_s)}$, where $\beta_i > 0$ for $i = 1,2,3$

* C_{max} denotes the nominal voltage of the battery.

3) Electro-thermal model

Electro-thermal Models (EtMs) are of paramount importance for battery internal temperature T_i estimation. In EtMs, the thermal behaviors are analogized and reproduced by electrical components. Two commonly used thermal models are depicted in Fig. 4. Fig. 4(a) is a second-order thermal model. Fig. 4(b) is the simplified second-order thermal model. With the thermal model, the battery internal temperature T_i can then be deduced with the power loss and ambient temperature. The accuracy of the T_i estimation mainly depends on the power loss. Table IV summarizes the expressions used for EtMs.

Table III Thermal and electrical parameter analogy

Thermal	Electrical
Temperature (K)	Voltage (V)
Heat flux (W)	Current (A)
Conductivity (W/K/m)	Conductivity (A/V/m)
Stored heat (J)	Storage charge (C)
Resistance (C/W)	Resistance (V/A)
Capacitance (J/C)	Capacitance (C/V)

This article has been accepted for publication in a future issue of this journal, but has not been fully edited. Content may change prior to final publication. Citation information: DOI 10.1109/TTE.2021.3135525, IEEE Transactions on Transportation Electrification

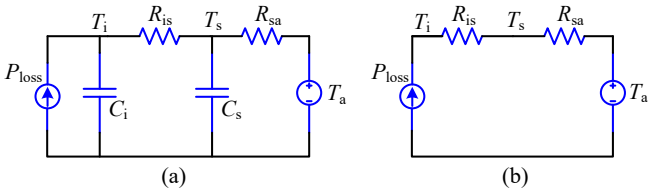

Fig. 4 EtMs. (a) Second-order thermal model [71]. (b) simplified second-order thermal model [72]. T_i is the battery internal temperature, T_s is the surface temperature, T_a is the ambient temperature. R_{is} and R_{sa} are the thermal resistance of the battery and the ambient, respectively. C_i and C_s are the thermal capacitance of the battery and the ambient, respectively.

TABLE IV EXPRESSIONS FOR COMMONLY-USED ETMS

Commonly-used EtMs	Expressions
Second-order thermal model [71]	$C_i \frac{dT_i}{dt} = P_{loss} - \frac{T_i - T_s}{R_{is}}$ $C_s \frac{dT_s}{dt} = \frac{T_i - T_s}{R_{is}} - \frac{T_s - T_a}{R_{sa}}$
Simplified second-order thermal model [76]	$T_i = T_a + P_{loss}R_{is} + P_{loss}R_{sa}$

Battery thermal distribution can be described by partial differential equations and boundary conditions [77-79]. A 3-dimensional thermal model is established in [79] to precisely emulate the thermal distribution of a pouch-type lithium-ion battery with partial differential equations. But the computational cost for solving the partial differential equation is too high for practical application. A mesoscale distributed electrothermal model is established in [80] to emulate the 3-dimensional thermal distribution of a cylindrical battery using finite element analysis. It is composed of a huge number of mesoscale lumped-thermal models that are connected in parallel. The heat generation distribution and temperature distribution inside the battery can be accurately emulated by the mesoscale distributed thermal model. Under the assumption that the temperature distribution of a cylindrical battery is uniform in the axial direction and circumferential direction, a simplified 1-dimensional distributed thermal model is formulated in [81, 82] to emulate the temperature distribution along the radial direction.

4) Aging model

Calendar aging and cycle aging are the two aging modes of LIB that reflect the degradation caused by storage and operation, respectively. Both aging modes can be described with empirical or semi-empirical models based on Arrhenius's law which depicts the dependence of the rate constant of a chemical reaction on major factors like temperature, activation energy [83, 84]. Some models have been summarized in [84, 85].

For calendar aging, the influential factors are temperature T, voltage V, and storage SoC [84, 86, 87]. Degradation during calendar aging accelerates at high voltage levels, high storage SoC, and high store temperature. The following models have been developed to describe calendar aging.

Considering the temperature effect, the capacities are fitted with (4) [88]:

$$Q = Be^{\left(\frac{-E}{RT}\right)}t^z \tag{4}$$

where B is the pre-exponential factor, t is the calendar aging time. z is constant.

In [89], both temperature and voltage are considered in capacity estimation with (5):

$$\frac{L_{cal}(t,T,V)}{L_0(t_0,T_0,V_0)} = 1 + C_T^{\frac{T-T_0}{\Delta T}} C_V^{\frac{V-V_0}{\Delta V}} c_a t^z \tag{5}$$

where L_{cal} and L_0 are the current and reference capacity degradation factor. t_0, T_0, V_0 are the calendar aging time, temperature, and voltage at reference condition, respectively. C_T, C_V, c_a are the aging coefficient for aging, temperature, and voltage. z is chosen as 0.5 with the assumption SEI formation is the dominant aging process.

In [90], the impact of SoC is included. The capacity loss is estimated with (6) where the temperature dependence f(T) is represented as (7) with Arrhenius's equation, and the SoC dependence is derived as (8) from reformulated Tafel equation since SEI formation is the dominant aging process.

$$Q = k_{ref} f(T) f(SoC) \sqrt{t} \tag{6}$$

where k_{ref} is a constant determined at the reference condition $SoC_{ref} = 50\%$, $T_{ref} = 298.15K$.

$$f(T) = e^{\frac{-E}{R}\left(\frac{1}{T} - \frac{1}{T_{ref}}\right)} \tag{7}$$

$$f(SoC) = e^{\left(\frac{\alpha F}{R}\frac{V_{ref} - V(SoC)}{T_{ref}}\right)} + k_0 \tag{8}$$

where V_{ref}, α, and k_0 are constants determined at reference condition.

Since many parameters, like charge throughput, SoC, cycling depth, temperature, and charging rate, may vary during cycling, cycle aging is more complicated. The following text shows the model development for cycle aging.

As the charge throughput Ah is proportional to time under CC cycling conditions [84], t is replaced with Ah in cycle aging for capacity estimation [91]. The impact of charging C-rate is studied with (9) in [91]. B is an exponential function of the C-rate as shown in (10) [92]. A similar model is expressed in [93].

$$Q = Be^{\frac{-31700 + 370.3C_{rate}}{RT}} Ah^z \tag{9}$$

$$\ln(B) = 1.226e^{-0.2797C_{rate}} + 0.9263 \tag{10}$$

Since SoC also influences the estimation, the pre-exponential factor is defined as a function of SoC (11) [94]:

$$Q = (\alpha SoC + \beta)e^{\left(\frac{-E + \eta C_{rate}}{RT}\right)} Ah^z \tag{11}$$

where α, β, η are constants.

The authors in [95] go further by examining the average SoC (SoC_{avg})and deviation of SoC (SoC_{dev})in a cycle. The capacity degradation is estimated by:

$$Q = \sum_{i}^{N} Be^{\left(\frac{-E}{R}\left(\frac{1}{T_i}-\frac{1}{T_{ref}}\right)\right)} Ah^{z} \tag{12}$$

$$B = k_1 SoC_{dev,i} e^{k_2 SoC_{avg,i}} + k_3 e^{k_4 SoC_{avg,i}} \tag{13}$$

where k_1, k_2, k_3, k_4 are constants. i is the cycle number.

In [96], degradation stress factors, temperature, discharge C-rate, charge C-rate, end of charge voltage V_{EoC}, and end of discharge voltage V_{EoD}, are fit separately with Arrhenius and Inverse Power Law models and then combined to account for the coupling between factors. Similar research is carried out in [97] where authors argued that the temperature characteristic is not exponential and then proposed a polynomial function as shown in (14). In addition, rather than using SoC_{avg} and SoC_{dev}, depth of discharge is employed. The authors also consider the charge and discharge current (I_{ch} and I_d) separately rather than one C-rate for both.

$$N(T) = k_1 T^3 + k_2 T^2 + k_3 T + k_4 \tag{14}$$

where k_1, k_2, k_3, k_4 are constants.

In [98], the battery is cycled under the vehicle operation scenario defined by the United States Advanced Battery Consortium. Apart from charging rate, temperature, and minimum SoC (SoC_{min}), an additional stress factor, the ratio between charge-depleting and charge-sustaining, is considered for capacity loss as:

$$Q = f(\cdot) e^{\left(\frac{-E}{RT}\right)} Ah^{z} \tag{15}$$

$$f(\cdot) = \alpha + \beta (Ratio)^{b} + \gamma (SoC_{\min} - SoC_0)^{c} \tag{16}$$

where α, β, γ, b, and c are constants.

To account for both calendar aging and cycle aging, the models are combined or directly applying one model to cover both aging modes. Authors in [70] adopt the model shown in (17), similar to (9), to account for both aging modes in ChgOp. A similar model is proposed in [76].

$$Q = Be^{\left(\frac{-E+\alpha|I|}{RT}\right)} Ah^{z} \tag{17}$$

where α is the aging coefficient caused by the current I. B is the pre-exponential factor.

Despite the capacity loss, the aging rate has also been derived for estimation [99]. The aging rate is defined as [100]:

$$r = Be^{\left(\frac{-E}{k_B T}\right)} \tag{18}$$

It can be noted that more parameters are included with the booming research outcomes in LIB characteristics. This helps to cover different influential factors and enhances the simulation accuracy. However, it should be mentioned that there will be notable estimation errors when the operation condition deviates from the test conditions. This is challenging for field application.

Charging, especially fast charging, as part of the cycling process has a profound influence on the batteries' lifespan. In general, high charging rates, too high or too low temperature, large cycle depth, and high charge end voltage will lead to fast degradation. Since these parameters could have a converse influence in accelerating the charging process, for instance, high charging rates are essential for fast charging, this forms the dilemma of an ideal charging approach.

5) Summary

In conclusion, EcMs manifest the physical awareness, for instance, kinetics and charge transfer, of LIB during charging which helps to diagnose AMs like lithium deposition. Therefore, EcM-based approaches are also referred to as 'white-box' approaches. However, the EcM is formulated with high-order partial differential equations, and thus it can be computational demanding for online applications. On the contrary, ECM is much more concise and aims to emulate the dominant electrical behavior of the battery. The drawback of ECM is that it does not provide any information regarding the battery's physical characteristics. EtM is analogous to ECM but incorporates the description of thermal properties. Attributed to the specific feature, the EtM- and ECM-based approaches are also referred to as 'grey-box' approaches. The aging model helps to estimate the State of Health (SoH) of LIB and is used to evaluate the charging approach [101]. In ChgOp techniques, multiple models might be combined to cover the designated aspects. These techniques are reviewed in Sections IV and V.

C. Aging mechanisms

During operation, Li-ions shuttles between 1) the solid electrodes, 2) Solid Electrolyte Interphase (SEI) and Cathode-Electrolyte Interphase (CEI), and 3) the electrolyte. Many AMs might appear during this process as shown in Fig. 5 which have been summarized by [102-104].

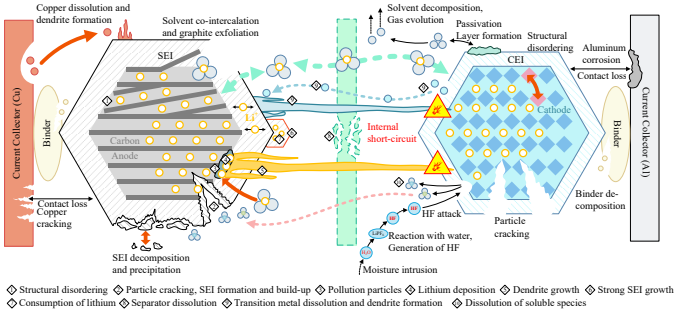

Fig. 5 Major AMs in LIB summarized and reproduced from [102-104].

The major aging mechanisms are SEI formation & crack & reconstruction [47, 51, 105-107] and lithium deposition [51, 108-113] on the anode side, and CEI layer formation & cracking [51, 102, 114, 115] on the cathode side. Apart from these, the shuttle of the Li-ion might also cause structure disordering and exfoliation [102, 116, 117], side reactions, like solvent co-intercalation, soluble species decomposition, and separator dissolution [110]. In addition, conducting salt (e.g. $LiPF_6$) can react with water from the environment leading to

deteriorated cell performance [110, 118]. Furthermore, contact loss might occur between the current collector, binder, and the electrode due to the corrosion of the aluminum current collector, binder decomposition, or copper dissolution & dendrite formation [102, 117, 119, 120]. This section provides an exhaustive illustration of three AMs that are frequently considered in ChgOp techniques.

1) SEI formation & crack & reconstruction

During the very first few cycles, due to the transmission of Li-ions between half electrodes via the electrolyte, SEI is formed at the interface of the electrolyte/anode [34, 47, 105, 114, 121]. SEI layer is built of decomposition products of electrolytes and Li-ions. The compositions of the SEI layer include LiF, Li_2CO_3, Li_2O, $ROCO_2Li$ [106, 114, 121]. This process stops when all the active area of the electrode is covered and the film stabilizes. During this process, there is a fraction of irreversible capacity loss due to the reduction of cyclable Li and exfoliation of the graphite structure [47].

During normal charge/discharge, the volumetric expansion and contraction of anode active particles cause cracks in the SEI layer [106]. Graphite at the crack will be exposed to electrolyte again and induces SEI reconstruction [102]. The reconstruction process is non-reversible and causes lithium inventory losses, which lead to battery capacity fade and power fade [51, 102]. Moreover, the SEI formation inevitably leads to electrolyte decomposition which causes battery impedance increment [102].

2) Lithium deposition

Due to the beneficial characteristics like the high specific capacity of 372 mAh g^{-1} [122] and stability [4, 123], and low cost, graphite-based material dominates the LIB anode material market. However, the equilibrium potential of graphite is very low and close to the voltage of lithium deposition/dissolution [51, 108, 109]. During charging, Li^+ intercalates with graphite in a narrow potential range. As shown in Fig. 6, with the evolvement of the intercalation, the potential changes from 0.35V versus Li^+/Li in the LiC_{72} stage to ~ 0.05V in the LiC_6 stage [124, 125]. With the progress of the intercalation process, the potential versus Li^+/Li decreases. When the potential drops to 0.065V, the intercalation process of the finite applied current saturates. Thus, when the potential is below 0.065V, there will be lithium deposition [126]. This is especially the case at high SoC which corresponds to low electrode potential [127]. Furthermore, the lithium deposition fosters lithium dendrite formation which eventually leads to internal short circuits and thermal runaway as shown in Fig. 5 [128].

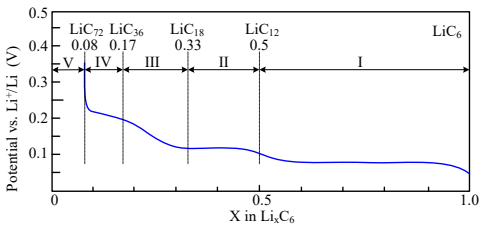

Fig. 6 The lithium-graphite intercalation compounds and corresponding potential [124, 125].

Lithium deposition is mainly associated with two processes, the charge transfer process and lithium diffusion process in the solid host material as shown in Fig. 6 [110]. Various limiting factors in both processes have been investigated to improve the charging C-rate while minimizing the lithium deposition [110, 129-131]. The charge transfer includes the transportation of Li-ions through the CEI layer, in the electrolyte, through the SEI layer, and to the border of the solid host material where an electron is accepted [129]. The resistance of this process is denoted as R_{ct} as described in (19) [129, 132].

$$\frac{1}{R_{ct}} = A_0 e^{(\frac{-E}{RT})} \tag{19}$$

where A_0 is a constant, E is the activation energy, R is the gas constant and T is the absolute temperature.

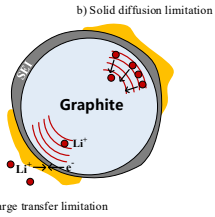

Fig. 7 Schematic illustration of Li deposition occurring at the surface of graphite particles. Reproduced from [110].

Take the LFP battery as an example, the limitation comes from the difference of the activation energy between the SEI and CEI layers. Since the SEI layer has a higher E compared with the CEI layer. Thus, in the full cell, transportation of Li-ions in the SEI layer is the limiting factor. A similar conclusion has been reached in [130] where extreme high current is applied to half cells and symmetric cells to identify the limiting factors. Moreover, the transportation of Li-ions in the SEI layer is also hampered at a lower temperature [133]. The additives in the electrolyte can also influence the transportation process [134]. The charging pulse rate has been maximized in [110] by considering the above-mentioned characteristics of the charge transfer process in an Electrochemical Model (EcM).

The performance of the lithium diffusion process can be represented by the diffusivity described in (20) [131].

$$D = D_0 e^{(\frac{-E}{k_B T})} \tag{20}$$

where D_0 diffusion coefficient, k_B is the Boltzmann constant.

Operational parameters that influence the lithium deposition include temperature, high charging C-rate, and cut-off voltage [131]. It is apparent that temperature plays a role as shown in (20). High charging C-rate causes Li-ion concentration gradient in the electrolyte which influences the diffusivity [135]. A high cut-off voltage or SoC leads to a high diffusion energy barrier E which impedes the diffusion process. In conclusion, lower temperature, high charging C-rate, and high SoC can cause accumulation of Li at or near the border of the anode which will block the diffusion path and lead to lithium deposition.

3) CEI formation & cracking

Similar to the SEI layer in the anode, there is a CEI layer formed at the interface of electrolyte/cathode [34, 47, 105, 114, 121]. The compositions of the CEI layer also include LiF, Li_2CO_3, Li_2O, $ROCO_2Li$ [106, 114, 121]. During the charging, the de-intercalation process in the cathode might introduce phase transition which leads to crystal structure disordering [102]. The thermo-instability of de-lithiated cathode material at high SoC is also problematic [102]. Depending on the cathode material, there is a different ratio of metal cations dissolved in the electrolyte [86, 103, 115]. Furthermore, CEI layer formation also induces electrolyte decomposition and gas evolution [102, 115] which causes the battery impedance increment and consequently power fade.

These three AMs are accelerated during fast charging. Thus, various optimization approaches are proposed to improve the charging speed, while minimizing the side effects. The following sections review the ChgOp approaches.

III. Charging Optimization System

The structure of the ChgOp system can be summarized as Fig. 8. The required data source is captured from the battery system and used in the optimization approaches. During the charging process, control variables are regulated to achieve the optimization objectives within the constraints. According to whether the algorithm dynamically adjusts the control variables or not, the ChgOp system is divided into open- and closed-loop ChgOp. In the open-loop ChgOp, the charging strategy is kept the same throughout the lifespan, while control variables are regulated to adapt to the operational variations in closed-loop ChgOp. The variations can be any electrical, thermal, or electrochemical changes of the battery, for instance, aging. In addition, optimization objectives in the open-loop system are succinct and not as critical as those in the closed-loop system.

Since data sources, optimization objectives, constraints, and control variables are shared in both systems. They are illustrated in this section followed by a review of parameters adopted in the latest research.

A. Data source

Data sources include direct measurements captured from the battery as well as derived parameters. Both are used as inputs for the optimization approach. For LIB, the direct measurements include charging current I_C [50, 70, 136], battery terminal voltage V_{Bat} [50], battery surface temperature T_s [56, 137], Electrochemical Impedance Spectroscopy (EIS) [138, 139], battery volume [140].

The derivative parameters include internal battery temperature T_i [71, 72, 76], battery charge capacity Q [50, 60], SoC [50, 56, 60, 70, 72, 74, 141], open-circuit voltage V_{OCV} [142, 143], incremental capacity dQ/dV [137]. In particular, the SoC is a critical intermediate variable that participated in the charge control, and a variety of techniques have been proposed in the literature for online SoC estimation [144-147]. Moreover, T_i is elevated due to heat generation, particularly at a high charge/discharge rate. Experiments have evidenced a temperature rise of 15℃ from the surface to the core of LIB [148]. These facts suggest that the *in-situ* measurement of T_i is critical for the charging control. Attributed to the recent research progresses, the *in-situ* measurement of T_i has been enabled by the use of embedded temperature sensors [149]. EtM-based estimation techniques can also be used to obtain an estimate of T_i [81, 150]. Unlike the SoC and T_i which are direct indicators for the charging control, the dQ/dV is an important variable of the incremental capacity analysis, which is typically used for LIB health diagnostic [151, 152]. However, it is also linked to the electrode material-level phase mitigation and over-potential, giving deep insights into the dynamical conditions inside the LIB during high-rate charging. Hence, this variable is also valuable to provide an important hint for the charging rate control.

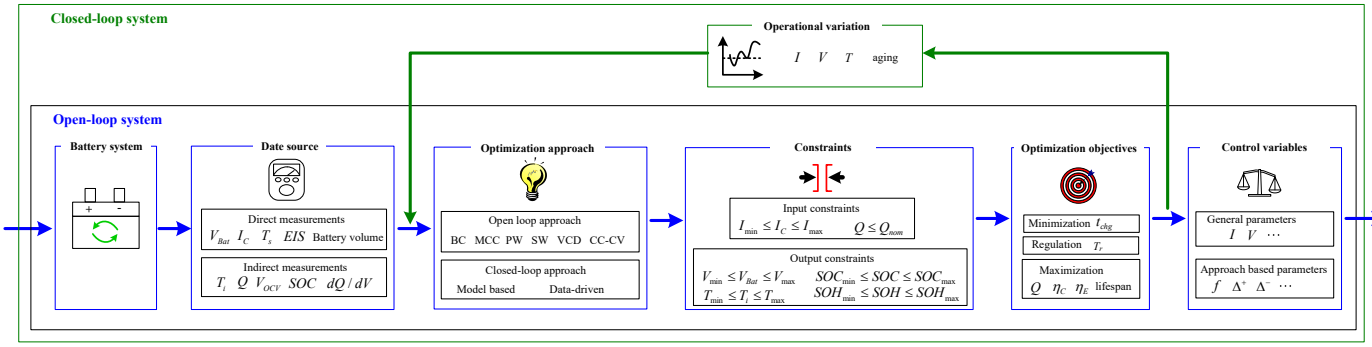

Fig. 8 Schematic diagram of the ChgOp system. I_{min} and I_{max} are the minimum and maximum charging current, respectively. Depending on the battery chemistry, I_{max} can be 4C or more. V_{min} and V_{max} are the minimum and maximum terminal voltage. T_{min} and T_{max} are the minimum and maximum internal battery temperatures.

Table V evaluates the data sources by the applicable scenario. The application scenario determines which application the charging approach is suitable for, real-time, *in-situ*, or offline. For practical application, data sources should be able to be captured in either *in-situ* or real-time scenarios. It can be noted that battery volume is not suitable for practical applications.

TABLE V COMPARISON OF DATA SOURCES

Parameter	Applicable scenario			Reference
	Offline	In-situ	Real-time	
I_C	✓	✓	✓	[50, 70, 136]
V_{Bat}	✓	✓	✓	[50]
T_s	✓	✓	✓	[56, 137]
EIS	✓	✓		[138, 139]
Battery volume	✓			[140]
T_i	✓	✓	✓	[71, 72, 76]
Q	✓	✓	✓	[50, 60]
SoC	✓	✓	✓	[50, 56, 60, 70, 72, 74, 141]
V_{OCV}	✓	✓	✓	[142, 143]
dQ/dV	✓	✓	✓	[137]

B. Optimization Problem Formulation

Optimization objectives are the critical parameters that influence the charging control strategy. Despite different selections in particular works, the prevalent optimization objectives can be generally summarized as charging time t_{chg} minimization [108, 153], charge capacity Q maximization [153], charge efficiency η_C maximization [153], energy efficiency η_E maximization, cycle life maximization [108], and temperature rise regulation [71]. Charge efficiency η_C is the ratio between charge extract from the battery during discharge and that stored to the battery during charging. Energy efficiency η_E is the ratio between the energy extracted from the battery when it is completely discharged and the energy consumed to fully charge the battery. t_{chg} can be measured with a timer. While evaluation of cycle life is more complicated, many parameters have been used as indicators [154, 155], for instance, remaining capacity [91, 156, 157], internal resistance [156, 158, 159], incremental capacity dQ/dV [160, 161], EIS [162], specified irreversible degradation modes [62]. These are vital parameters for the charging process.

The prestigious benefit of optimized charging control is the simultaneous regulation of control variables to meet critical demands of quick refueling and less impact on battery safety and aging. In general, control variables can be the charging current [71] or charging voltage [143], depending on the specific charging mode. However, the actual parameters might take different forms depending on the charging strategy, for instance, it can be pulse frequency, duty ratio, etc.

An efficient definition of the constraints is essential to ensure the safe and healthy operation of the battery while achieving the optimization objectives. The constraints are divided into two categories according to their function, i.e., input constraints and output constraints. Explicitly, input constraints are placed on input parameters, including the charging current I_C [56, 57, 60, 62, 70, 72, 74, 141, 163] and charge capacity Q [50, 60]. Output constrains are defined for battery terminal voltage V_{Bat} [56, 57, 60, 62, 70, 72, 74, 141, 163], internal battery temperature T_i [57, 70, 72], SoC [50, 56, 60, 70, 72, 74, 141], and State of Health (SoH) [70]. Such constraints can be either hard boundary or soft one with reasonable penalty once violated. With a well-formulated optimization problem-oriented for battery charging, a considerable number of optimization approaches have been proposed in the literature to enhance the charging performance. They are summarized in Section IV and V as open-loop ChgOp and closed-loop ChgOp, respectively. Optimization approach associated constraints and control variables vary with the ChgOp techniques. Thus, they are illustrated individually in Sections IV and V.

IV. Open-loop Charging Optimization

For LIB charging, open-loop optimization is mainly profile-based approach where a superior charging profile is proposed and applied to the battery throughout the lifespan without considering any variation (e.g. aging) during the cycling.

A. Boost Charging

Authors in [9] first proposed boost charging as shown in Fig. 9. During boost charging, the battery voltage is kept at V_{Bst}, while the current drops rapidly with the maximum current limited to I_{max}. Under extreme cases, when V_{Bst} is so high that the current hits I_{max} and remains I_{max} the whole phase, the charging profile turns to high C-rate CC.

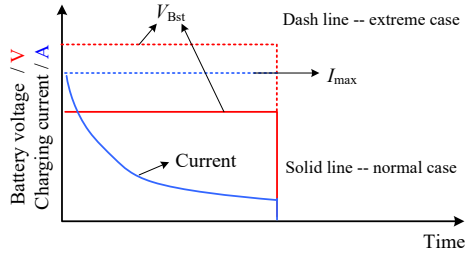

Fig. 9 Boost charging profiles.

In [9], the battery charged with the boost charging-CC-CV profile is compared with that charged by traditional CV and CC-CV charging approaches. The results demonstrated that CV charging can cause server degradation especially when the voltage is set higher than 4.2V. However, the boost charging phase reduces the charging time without introducing any extra degradation effects. This observation is challenged by [127] where two CC phases and one CV phase is employed at different SoCs and compared with CC-CV. Results suggested that degradation appears at both very high and very low SoC. Proper SoC selection only lessens degradation caused by the boost charging phase. Some researchers believed that boost charging should be applied at low SoC [164, 165]. Because the concentration gradient between the electrolyte and the graphite anode is large at low SoC which enables the high current density [164, 165].

B. Multi-stage Constant Current charging

Multi-stage Constant Current charging (MCC) charging generally consists of two or more CC stages and each stage is assigned a different current value. As shown in Fig. 10, there are n stages, and the current level assigned for the i^{th} stage is I_{chi} (i=1, …, n). Initially, since V_{MCC1}=V_{MCC2}=…=V_{MCCn}=V_{max}, I_{chi} satisfies $I_i \geqslant I_j$, if i<j, i, j =1, …, n, which means monotonically decreasing current level [75, 166]. Later, it generally refers to multiple CC charging phases without constraints regarding voltage/current level. The suggested number of charging stages

is no more than 5 because further increment in the charging stage only achieves a negligible effect in reducing the charging time [70].

MCC has been combined with CC and CV which results in CC-MCC [73, 75, 127, 166-168] and MCC-CV [49, 169-171] charging protocol. Authors in [172] applied MCC throughout Phase II and Phase III. Results show that MCC promotes fast charging because a significant amount of charge is obtained in the high current charging phase and the gradual decrement reduces the time to full charge. Other research also showed that MCC supports avoiding severe temperature rise and extends cycle life [31].

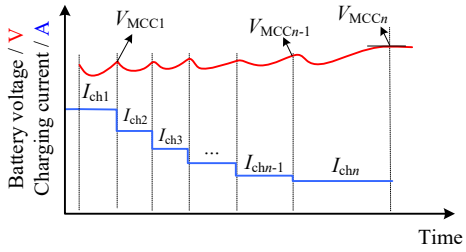

Fig. 10 MCC charging profiles.

A five-stage MCC approach is optimized in [73, 168]. The current level of MCC is determined with the assistance of the ECM shown in Fig. 3(c). The 1st current level I_1 is the same as the CC phase. The 5th current level I_5 is determined with (21), the 2nd, 3rd, and 4th current levels I_2, I_3, I_4 are determined with (22). The influence of the cut-off voltage V_{max} on the charging performance is also studied. The results show that the proposed CC-MCC charging approach can enhance the charging speed, charge efficiency, and charging energy by 11.9%, 0.54%, and 1.8%, respectively.

$$I_5 = \frac{1}{R_{eq}}(V_{\max} - V_{s,1}) - \frac{3600}{C_{eq}R_{eq}}Q_{nom} \tag{21}$$

$$I_2 = \sqrt{I_1 I_3} \quad I_3 = \sqrt{I_2 I_4} = \sqrt{I_1 I_5} \quad I_4 = \sqrt{I_3 I_5} \tag{22}$$

where V_{S1} is the voltage for the first CC stage. Q_{nom} is the nominal capacity.

In [109], a three-stage MCC is investigated where the stages are determined by SoC. The three stages are SoC at 0-0.3, 0.3-0.6, 0.6-0.8. In total, thirteen charging patterns with different C-rates are investigated. Among them, the 2.2C-1.9C-0.9C charging profile has the best performance.

The abovementioned works optimize the MCC profile by means of enumeration. This process is time-consuming and the solution might be trapped at a local optimum. To improve the efficiency, Taguchi orthogonal arrays are introduced to the MCC optimizations [75, 166, 173]. Taguchi approach aims to optimize the design of experiments with the least cost of experimental effort. It studies the impact of selected variables on the response and optimizes the procedure by a limited number of trial tests. Furthermore, it is a fractional factorial design that has considerably fewer trial numbers when compared with full factorial designs. In general, it contains five steps, namely factor selection, orthogonal array allocation, trial tests, analysis, and confirmation tests [75, 166, 173]. First, variables are selected and the corresponding level number is determined. Then, with these parameters, the suitable orthogonal array can be chosen. After that, trail tests are designed according to the orthogonal array. And the trial test results are analyzed to find the optimum conditions. For the analysis, there are mainly five approaches, namely, analysis of variance, the total sum of squares, the residual sum of squares, analysis of means, signal to noise ratio (S/N). S/N is the most prevalent approach and is defined as (23) and (24) [174]. Finally, confirmation tests are carried out to verify the analysis.

$$\frac{S}{N} = \begin{cases} -10\log(n^{-1}\sum_i Y_{ij}^{-2}) & larger\ the\ better \\ -10\log(n^{-1}\sum_i Y_{ij}^{2}) & smaller\ the\ better \end{cases} \tag{23}$$

$$\frac{S}{N} = 10\log(\frac{\overline{Y}^2}{(n-1)^{-1}\sum_i (Y_{ij}-\overline{Y})^2}) \tag{24}$$

$$\overline{Y} = n^{-1}\sum_i Y_{ij} \tag{25}$$

where, i, j refers to the output i^{th} row j^{th} column. Y is the selected variable.

In [75, 166], Taguchi orthogonal array-based approach is applied to find the optimal five-stage MCC charging pattern. The results showed that the optimized MCC approach reduces charging time and prolongs cycle life by 11.2% and 57%, respectively.

C. *Pulse Wave charging*

Both Sinusoidal Wave (SW) and square wave charging processes have been referred to as pulse charging. Herein Pulse Wave (PW) charging particularly refers to the charging process in which a square wave is used as shown in Fig. 11. SW charging is summarized separately.

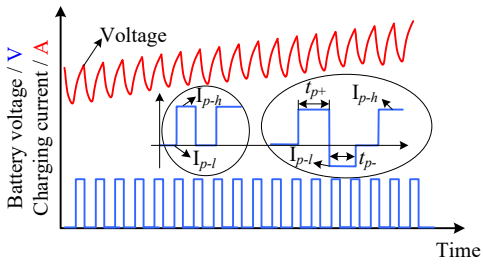

Fig. 11 PW charging profiles. t_{p+} is the pulse length of I_{p-h} and t_{p-} is the pulse length of I_{p-l}. The duty ratio of I_{p-h} Δ^+ is the ratio between t_{p+} and the total period of the pulse. The duty ratio of I_{p-l} Δ^- is the ratio between t_{p-} and the total period of the pulse.

PW charging is implemented by injecting the current pulse into the battery. I_{p-h} and I_{p-l} refer to the high and low current level of the pulse, $I_{p-h}>I_{p-l}$. The parameters that define the waveform are I_{p-h}, I_{p-l}, the duty ratio of I_{p-h} Δ^+, the duty ratio of I_{p-l} Δ^-, and frequency. In Fig. 11, the two major forms of the pulse are shown as insets which correspond to $I_{p-l} \geqslant 0$ and $I_{p-l} < 0$, respectively.

PW has been thoroughly investigated for lead-acid batteries

[175] and later introduced to LIBs due to its impact on the Li-ion concentration. It is believed that the short break, or off period, contributes to the evener ion concentration and slower polarization [176]. In [176], PW-CV charging is investigated for capacity retention improvement based on the P2D model with thermal effect considered. The results demonstrate that, with the same average current, PW-CV causes lower temperature variation and prolongs lifetime by decreasing polarization and the SEI layer growth.

There are also antithetical propositions regarding the impact of PW. As reported in [177], it is believed that PW only influences the superficial regions of the electrode, but does not influence the average concentration profile which is determined by the average current. There is also severe capacity decrement caused by PW as reported in [177]. In [178], it is reported that pulses shorter than milliseconds are buffered by the large double-layer capacitances at the electrode/electrolyte interfaces. The impact on concentration is not effective until the duration of PW is in the range of second.

The influence of PW on charging speed is also debatable. Due to the short break, the time for PW charging would be longer compared with CC charging with the same average current. Furthermore, with the same average current, PW tends to have a higher root mean square value, this is especially the case for PW charging with a negative pulse, which causes extra energy losses and consequently aggravates thermal effects [165, 176]. When the magnitude of the applied current is high, the battery opts to reach the cut-off voltage prematurely [165]. Relevant works also indicated that the effect of PW varies with SoC. At high SoC, PW can lead to temperature rise, which is beneficial for ion diffusion but facilitates capacity loss.

To optimize the performance of PW charging, research is carried out by tuning the PW parameters like the duty ratio of the positive pulse [179-181], the amplitude of positive pulse [180-183], the duty ratio of the negative pulse [165], amplitude of negative pulse [182, 183], frequency (500Hz, 1000Hz, 2000Hz [179]). In [165, 179, 184], the performance of PW and CC are similar to each other. In [181], PW with CC amplitudes but monotone increasing resting time shows better performance due to reduced concentration over-potential. Extreme high amplitude (15C) of positive/negative pulse is applied in [182, 183] which causes a drastic increase of SEI layer and hence the impedance. With higher frequency, the battery shows a lower temperature increment compared with CC with the same average current [165]. Researchers in [184] optimize the charging process by tuning the negative pulse width, which is determined according to SoC. The experiment shows that the negative pulse has a similar or a bit worse performance compared with the CC-CV approach.

To simplify the optimization process, Taguchi orthogonal arrays have also been applied to PW approaches to tune waveform relevant parameters. In [174, 185], the impacts of duty ratio, frequency, and ambient temperature are investigated. The results show that, with optimized PW, charging time is reduced by 47.6%, and charge efficiency and energy efficiency are increased by 1.5% and 11.3%, respectively.

D. Sinusoidal Wave charging

SW charging uses a sinusoidal current with a DC bias [186]. The parameters that define the waveform are the amplitude of DC bias, the amplitude of the SW, and the frequency of the SW. SW charging, also known as sinusoidal ripple current charging, is introduced to charge LIB at the frequency where the battery impedance reaches a minimum. This means the energy loss is minimized during charging and the energy transfer efficiency is maximized [187, 188].

As reported in [187, 188], the charging performance of LIB was improved by using SW charging at the frequency of 998 Hz which minimizes the AC impedance. Compared with CC-CV charging, SW charging in these works show enhanced performance regarding the charging time, charging efficiency, temperature build-up, and lifespan extension. Experimental results show lifetime improvement by 17%, 1.9%, 45.8%, and 16.1%, respectively. The importance of the DC component in the SW charging has been discussed in [138]. Results show that the SW-CV method has the fastest charging speed with the same average current. However, due to the existence of a sinusoidal component, the RMS current of the SW-CV is higher which causes an 18% increment of the maximum temperature. This is highly desired for low-temperature charging, but can be quite unfavorable for medium- or high-temperature charging since the additional temperature build-up can lead to the catastrophic thermal run-away problem. Other drawbacks of the SW-CV implementation include high cost, large size, protection complexity, and audible noise associated with the inclusion of AC excitation equipment [138]. The conclusions in [138, 187, 188] are also challenged by authors in [189], where the performance of SW, triangular wave, and PW charging are compared with the CC charging. The results show that the CC approach has the highest energy efficiency, shortest charging time, and lowest temperature increment. However, the average currents of these four charging approaches are not the same, which makes the conclusion skeptical.

The detrimental impact of the SW approach has also been reported. In [190], the LFP battery was cycled with SW at 120Hz for about 2000 cycles. The results show that the SW approach has higher capacity degradation and lower energy efficiency compared with the CC protocol. It is concluded that the SW is an alternative approach for battery charging when considering the better efficiency of the converter.

Various approaches have been introduced to optimize SW charging. In [191], SW with negative pulses is proposed to remove the formed passivation layer and to revive the loss of lithium. In the first test, this approach is applied to batteries at different SoH levels. Results show that the capacities of the three batteries increase from 64.7%, 78.8%, and 84.9% to 83.4%, 88.3%, and 89.1%, respectively, and remain at the high level which verifies the effectiveness of reviving aged cells. In the second test, the proposed approach and traditional CC-CV approach are applied to fresh cells. Results show that, after 600

cycles, the battery charged with the proposed approach has 14.5% more capacity than that charged with the CC-CV approach.

E. Customized charging approaches

A Varying Current Decay (VCD) protocol is proposed in [192]. Rather than CC, the charging current varies according to predefined empirical equations. In this paper, the VCD is defined as a short current pulse followed by a current decay in the form of (35). This is to adapt to the characteristics of LIB in different SoC regimes as illustrated in Section II-A.

$$I = (I_0 + k_1 t^{0.5}) / (1 + k_2 t^{0.5} + k_3 t) \quad (26)$$

where k_1, k_2, k_3 are constants, I_0 is the initial current, t is time.

This charging protocol is compared with CC-CV and CV charging. Results show that the VCD protocol improves the charging speed and capacity utilization, but introduces faster degradation during cycling. With the EIS and Scanning Electron Microscope analysis, the capacity reduction is mainly due to the increased film formation on carbon electrodes caused by voltage peaks during the transition from current pulse to current decay.

In [100], the traditional CC-CV charging is optimized by imposing constraints on the anode potential. The optimized charging strategy is determined in such a way that the lithium deposition is prohibited at low temperature (25°C) and high SoC. The results show that by adding this constraint, the lifespan of the LIB is doubled compared with its counterpart where anode potential is ignored. In [140], the relationship between the capacity loss/lithium deposition and the maximum/mean irreversible volume change is accessed with a bivariate correlation. The results show that lithium deposition will cause irreversible volume expansion. A look-up table is generated for irreversible volume expansion at various C-rates and SoC. On this premise, the MCC approach is optimized by limiting the maximum volume expansion, or equivalently, the lithium deposition. Following this endeavor, the maximum allowable C-rate can be determined for a given SoC. A comparative study among three cells shows that the proposed method achieves 11% charging time reduction and about 20% extension of lifespan.

TABLE VI SUMMARY AND COMPARISON OF VARIOUS CHARGING PROFILES

Ref.	Phase I & II	Phase III	Battery type	Charging time	Temperature	Charge efficiency	Lifespan
[9]	Boost charging-CC	CV	US18500	+20%	+7.5°C	NA	-4%
[49]	MCC	CV	LFP	-71%	NA	NA	NA
[138]	SW	SW	NA	-9,7%	+8.5%%	NA	NA
[140]	MCC	CV	LCO/NMC	-11%	NA	NA	+20%
[174]	PW	PW	LiPo	47.6%	+1°C	+1.5%	+25%
[75, 166]	MCC	MCC	LMO	-11.2%	-(0-0.5)°C	+1.02%	+57%
[167]	MCC-PC	MCC-PC	NA	-22%	-(0-0.5)°C	NA	NA
[73, 168]	CC	MCC	ICR18650	-12%	-1°C	+0.54%	NA
[171]	MCC	MCC	LiPB	22.5%	-(1-1.5)°C	NA	NA
[176]	PW	CV	LFP	0%	-2.66°C	NA	+0.2%
[177, 193]	PW	PW	LFP	NA	+(5-10)°C	NA	NA
[188]	SW	SW	UR18650W	17%	-2°C	2%	+16.1%
[189]	SW	SW	NMC	+0.67%	+0.02°C	NA	NA
[190]	SW	CV	LFP	NA	+0.2°C	-1.5%	-1.2%

+: Increment in charging time/temperature/charging efficiency/lifespan.
-: Decrement in charging time/temperature/charging efficiency/lifespan.
NA: No information is provided or not applicable.

F. Summary

Some representative open-loop ChgOp techniques are compared again in Table VI regarding the charging time, temperature rise, charge efficiency, and life impact. It is noted that MCC-CV proposed in [49] shows the best performance regarding charging time reduction, 71% reduction compared with CC-CV. Drastically lifespan increment is obtained in [75, 166] with MCC-MCC charging. However, the impact of MCC-based charging profiles on the temperature and charge efficiency improvement is trivial. The best temperature performance is captured in [176], where PW-CV helps to achieve 2.66°C temperature reduction. Moreover, 2% improvement is observed in [188] regarding charging efficiency.

V. CLOSED-LOOP CHARGING OPTIMIZATION

Unlike the open-loop system, the response or output is continuously fed back to the system so that the charging approach is regulated dynamically in the case of a closed-loop ChgOp system. In this way, the charging process is adapted to operational variations like temperature and aging. Referring to the state-of-the-art progress, the closed-loop optimization approaches can be further classified into model-based and data-driven approaches. In this paper, model-based approaches refer to the collection of approaches where one or more battery models, such as electrochemical model, electrical equivalent circuit model, electro-thermal model and aging models, are employed to simulate the specified battery characteristics to assist the charging optimization. On the other hand, data-driven approaches don't use any models but extract the interested

battery characteristics from the data acquired beforehand or during the operation. This section gives an overview of these studies followed by an explanation of the analysis approach.

A.Model-based approaches

Model-based approaches are grouped in three categories according to the models used, namely, 1) ECM and ECM+EtM based approaches, 2) EcM and EcM+EtM based approaches, 3) EtM based approach.

1)ECM and ECM+EtM based approaches

ECM and ECM+EtM models are frequently applied to the optimization of charging profiles in Section IV. For instance, ECM+EtM based approaches are proposed to optimize the MCC charging process by numerical methods like Particle Swarm Optimizer (PSO) [70] and the ensemble multi-Objective Biogeography-based Optimization (mOBGG) [72]. In [70], PSO is applied to balance the charging time and aging. The results show that the duration of balanced charging is reduced by 43.4% with the negligible battery SoH decrement. Results in [72] show that the capacity loss of MCC-CV charging reduces by 16.5% compared with CC-CV.

Control strategies have also been adopted for charging optimization [70, 74, 194, 195]. Representative control strategies include explicit Model Predictive Control (MPC) [74] and Fuzzy control [194]. In [74], MPC enables online optimization with multi-segment linearization applied to the ECM in Fig. 3(d). However, the constrained optimization problem is solved offline and expressed as piecewise affine functions for online or real-time applications. In [194], the relationship between charge polarization voltage and current & SoC is analyzed and quantified based on the *n*-order RC model in Fig. 3(b). The quantified relationship is then used as a guideline to optimize the charging process at different SoCs. The proposed approach achieves a balance between the charging time and aging. The same problem is addressed in [195], where the optimization between charging time and aging is implemented via pulse amplitude/width modulation charging with the history of battery operation considered.

Furthermore, there are also customized charging protocols developed based on ECM and ECM+EtM models [50, 71]. The Universal Voltage Control Protocol (UVP) is reported in [50] where the charging voltage is adjusted. In particular, an ECM model is built based on the data from pre-tests. The varying voltage profile is derived by accommodating the battery impedance with a Genetic algorithm. Since aging is also considered in the model, UVP has good performance throughout the lifespan of the battery. The results show that UVP enhances the lifespan by a 275% increment. The difference between VCD and UVP is that VCD uses the empirical equations to shorten the charging time while minimizing the impact on lifespan. UVP intends to provide a universal charging protocol that is independent on aging while maximizing efficiency in a designated charging time frame. In [71], a Constant Temperature-Constant Voltage (CT-CV) charging technique is proposed. The CT phase includes a CC phase and an exponential decay phase, in which the charging current is adjusted dynamically with a PID controller to keep the cell temperature below the predefined threshold while optimizing the charging current. The proposed CT-CV approach achieves an 18% charging time reduction.

Due to the simplicity of the ECM model, some approaches have been developed into customized chargers. In [196], a voltage pulse charger is developed. The average charge current is derived with (27). It is believed that by maximizing the $i_o D_n$, both the charging speed and charge efficiency can be improved.

$$i_{b,n} = k \cdot i_{o,n} \cdot \frac{T}{2\tau} \cdot D_n^2 \tag{27}$$

where k is a constant, T is the period of the pulse. $i_{o,n}$ is the exchange current density with duty D_n and τ is the transfer time constant.

In the experiment, the charging process is divided into full-charge detection mode, sense mode, and charge mode. The optimized duty ratio is determined during the sense mode and applied in charge mode. The results show that both charging speed and charge efficiency are improved compared with CC-CV charging by about 14% and 3.4%, respectively. Similarly, optimization of the pulse frequency is studied in [197] where the pulse frequency is varied so that the battery is charged in the minimum impedance regime. It shows that the charging speed of the proposed method is improved by 24% compared with CC-CV charging. Both frequency and duty ratio are considered in [198] where a pulse-based fast Internet of Thing charger is designed for multiple distributed battery cells. Compared with CC-CV, the proposed charging method achieves an 18.6% charging time reduction with a 3°C temperature increment.

Besides the pulse chargers, compact microchips have also been developed to improve the CC-CV charging speed. These chargers focus on the compensation of voltage drop V_{BiR} across the Built-in Resistance (BiR) [199-201]. The BiR includes external resistance from contacts, fuses, trace wires in the printed circuit board, and the internal resistance of the battery. Due to the voltage drop V_{BiR}, CC charging phase is shortened which extends the CV charging phase and consequently expands the overall charging time. By continuously detecting the BiR and compensating V_{BiR} with the appropriate transition voltage from CC to CV, the charging time in [199], [200], and [201] reduces 45%, 17.1%, and 13.5%, respectively. Authors in [202] go one step further by studying the impact of different compensation rates (0% to 100%) on temperature. 100% means full compensation of V_{BiR} and 0% means no compensation which also equals conventional CC-CV. It shows a higher compensation rate leads to faster charging but introduces high battery temperature which causes fast aging. Forced ventilation is required to balance the charging speed and temperature rise.

In general, since ECM is concise and provides a good reflection of the electrical characteristics of the battery, it is favored for charging optimization in both research and practical application. The major challenge of this is the online

optimization for the nonlinear ECM model. Overall, as summarized in Table VII Comparison of ECM and ECM+EtM model-based approaches, the ECM model with GA optimization in [50] shows the best performance regarding lifespan extension, 275%. The fast charging time is achieved with BiR compensation in [202], however, the lifespan reduces about 77.8%.

TABLE VII Comparison of ECM and ECM+EtM model-based approaches

Ref.	Battery type	Model	Optimization approach	t_{Chg}	T_{Bat}	η_C	Lifespan
[50]	LCO+NMC	ECM	Genetic algorithm	NA	NA	+1%	+275%
[70]	NCA	ECM+EtM	PSO	-43.4%	+0.6°C	NA	-4.8%
[71]	NCA	ECM+EtM	PID	-18.2%	-1.9°C	NA	NA
[72]	LFP	ECM+EtM	mOBGG	+1.7%	NA	NA	+5.2%
[200]	NA	ECM	BiR compensation	-17.1%	NA	NA	NA
[194]	$LiMn_2O_4$	ECM	Fuzzy control	+33.3%	+6°C	NA	+2%
[196]	NA	ECM	NA	-14%	NA	3.4%	NA
[201]	NA	ECM	NA	-13.5%	NA	NA	NA
[202]	LFP	ECM	BiR compensation	-47.9%	+11°C	NA	-77.8%

NA: No information or not applicable.

2) EcM and EcM+EtM based approaches

The superiority of EcM based approaches is that it reveals the battery's physical properties. Hence, many works spring up to exploit the EcM regarding fast [56, 57, 60, 62, 203-207] and health-conscious charging [57, 60, 62, 203-207] of LIB. In [56], a P2D model-based approach is leveraged to minimize the charging time. Quadratic Dynamic Matrix Control (QDMC) is improved to solve the multi-input multi-output optimization problem. In this approach, hard constraints are placed for the input parameters and soft constraints are used for output parameters to maximize the performance. The results show that charging time reduces by 34.3%.

Besides fast charging, the prevention of the major AMs – lithium deposition [57, 60, 62, 203-207] and side reaction [57] – have also been studied. In [60, 203], the 1-D EcM model is simulated in a closed-loop fashion to suppress the lithium disposition. Following the modeling, different optimization approaches are applied. Illustratively, Pontryagin's principle is used in [203], while nonlinear MPC is applied in [60]. The results show that the charging time is reduced by 11.9% and 50%, respectively. However, the battery temperature increases by 15°C in [60]. It should be pointed out that only simulation is carried out in [56, 60, 203].

The EcM-based approaches have been verified with experimental tests in [57, 62, 204, 207]. In [57], the linear time-varying MPC is applied to address the optimization considering thermal characteristics. The proposed charging approach could charge the battery in about 13min which is 22% less than CC-CV with no extra temperature increment. In [207], a nondestructive charging algorithm is proposed based on a simplified P2D model. The fast charging algorithm measures the anode over-potential to determine the status of the lithium deposition and then the charging current is modified accordingly. In comparison with CC-CV, the charging capacity of the proposed method is 3% less, while the charging time reduces 26.4% with no lithium deposition. In [204], the aging characteristic is considered, and a dynamic programming method is used to address the dual-objective optimization problem regarding charging time and battery degradation. Comparisons with CC-CV, health-conscious fast charging reduces charging time significantly by 45.5% with negligible impact on lifespan. Except for suppressing lithium deposition, authors in [62] further facilitate lithium stripping which helps to recover the lost capacity. A Reduced-Order electrochemical Model (ROM) is proposed by considering both lithium deposition and lithium stripping. The results are used to guide the selection of negative pulses to stimulate lithium stripping. The proposed method is able to reduce the charging time by 11.4%, with a drastic improvement in lifespan by 12.9%.

Table VIII Comparison of EcM and EcM+EtM based approaches

Ref.	Battery type	Model	Optimization approach	AM	t_{Chg}	T_{Bat}(°C)	Lifespan
[56]	Simulation only	P2D	QDMC	NA	-34.3%	NA	NA
[60]	Simulation only	1D-EcM	nonlinear MPC	Lithium deposition	-50%	+15	NA
[62]	NA	ROM	NA	Side reaction & Lithium deposition	-11.4%	NA	+12.9%
[57]	LFP	SPM	linear time-varying MPC	Lithium deposition	-22%	0	NA
[203]	LOC - simulation	1D EcM	Pontryagin's principle	Lithium deposition	-11.9%	NA	NA
[204]	LFP	SPM	Dynamic programming	Lithium deposition	-45.5%	NA	-1%
[207]	NMC	Simplified P2D	NA	Lithium deposition	-26.4%	NA	NA

NA: No information or not applicable.

Apart from the major AMs, some specific characteristics like stress [136] and cell design [153] have also been investigated. In [136], a nonlinear current charging approach is investigated where the current decays exponentially. An EcM is developed to optimize the charging profile and limit the charging stresses. The proposed charging protocol has superior performance compared with MCC.

Table VIII compares the performance of these approaches. Due to the complexity of the EcM model, some proposed models are only tested in simulation. Among these simulation research, the best performance is obtained with 1D-EcM in [60] where the charging time plunges by 50%, the highest among all the studies. However, this also introduces 15°C temperature rise. The best experimental performance is captured with SPM in [204] where the charging time declines drastically by 45.5%.

The longest lifespan, 12.9% increment, is achieved with ROM in [59]. It should be pointed out that there are only limited data regarding temperature and lifespan.

3) EtM based approach

The EtM has also been used to optimize the charging of LIB. In [137], the charging process is divided into ten steps according to the SoC level. The charging current is optimized according to charging time and the temperature rise. The temperature rise is estimated by a proposed enhanced thermal model. The optimization process is implemented with a Genetic algorithm by considering:

$$\begin{cases} F(t,\Delta T)=\alpha f(t)+\beta f(\Delta T) \\ \alpha+\beta=1 \end{cases} \tag{28}$$

where t is the charging time, ΔT is the temperature rise, α and β are the weight coefficients.

Moreover, various combinations of weighting coefficients are investigated. The optimized charging profile accelerates the charging speed by 7.6% with a similar temperature rise compared with CC-CV.

B. Data-driven approaches

Data-driven approaches, which treat the battery as a black-box system, have been widely explored in recent years for both the production and management of LIBs. A powerful framework has been proposed to quantify the feature importance of interpretable machine learning, which well benefits battery smart manufacturing [208]. With respect to the charge control, typically, a database comprising different charging actions and the corresponding performance is measured and analyzed, and afterward, the optimized strategy can be extracted with suitable algorithms. In [209, 210], data-driven approaches are proposed for the optimization of the MCC charging. In [209], the PSO-based Fuzzy control approach is derived. The results show that charging time, life cycle, and charge efficiency are ameliorated by 56.8%, 21%, and 0.4%. A machine learning approach is proposed in [210] to optimize the MCC approach aiming to reduce the experimental effort. In this work, an early prediction model is applied which could predict the end of life cycle number of a battery with only the first 100-life-cycle data and thus reduces the time of each experiment by 80%-90%. Along with the prediction model, a Bayesian optimization approach is proposed to estimate and explore among all the protocols and output only the potential superior ones, which has a longer lifespan. In this research, only 107 protocols, out of 224, need to be accessed to recognize the best ones. While it should be noted pre-tests are required, in this case, there are datasets from 41 batteries cycled to failure.

In [211], extensive tests are carried out with LIBs at different depths of discharge, currents, and temperatures. With a large amount of data, a battery aging model is formulated with the help of piecewise linear functions and a recursive Douglas Peucker line simplification algorithm. This data-driven aging model is then applied for ChgOp. The results show that there is a 6.39% improvement regarding battery degradation with the proposed approach and it brings financial benefit.

Most recently, Reinforcement Learning (RL), which is an emerging technique targeted for solving high-dimensional and complex optimization problems, has been introduced for LIB fast charging control. A representative work is reported in [212], where an electro-thermal-aging coupled model is built to describe the multi-physics property of LIB during high C-rate charging. Leveraging the model, a Deep Reinforcement Learning (DRL) strategy is trained offline and subsequently applied for online ChgOp, with considerations of the charging speed, the thermal safety (temperature build-up), and aging protection. A general framework of the proposed DRL-based fast charging strategy is shown schematically in Fig. 11. The illustrated strategy has been validated by both short-term charging experiments and long-term aging tests. Experimental results suggest that the LIB can be fully charged within 926s without violating the physical constraints by using the DRL strategy. Compared to the 6C CCCV strategy, the DRL strategy extends the LIB lifetime by 14.8% with an equivalent charging speed.

Within a similar RL-based framework, the EcM has been used for the fast charging of LIB in [213, 214]. The merit of such a deep RL-based strategy is rooted in the fact that the complicated optimization process is transmitted to the offline training stage, and the trained policy can be implemented in real-time attributed to the low computational demand. The use of RL for complex system optimization has also been explored in other relevant fields, like the energy management of hybrid electric vehicles [215, 216]. It is worth noting that such RL-based techniques can work without battery modeling, provided that sufficient real-world charging data are available to support the exploration process of RL. Furthermore, such strategies will better show their merits within the digital twin or cloud-based architecture, where the charging policy can be updated within the cloud using the incoming charging information, while the generated policy is used to guide the charging of the battery.

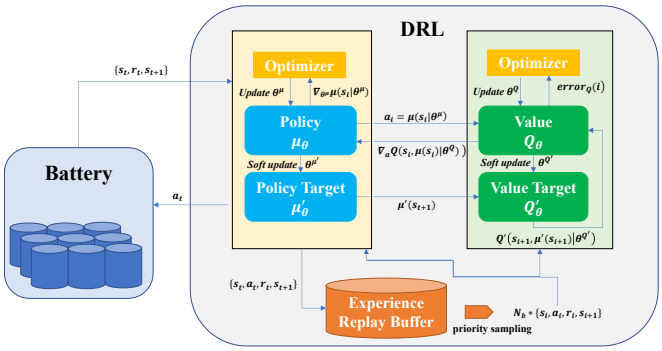

Fig. 12 DRL-enabled fast charging strategy.

It can be noted that a large amount of data is required in data-driven approaches. This consumes not only a large amount of computation power but also additional time to collect the data. However, since data-driven approaches treat the battery as a black-box system, it decreases the requirement of professional knowledge for instance battery chemistry. In addition, unlike model-based approaches, indicators in data-driven approaches

could reflect the battery characteristics but do not have any physical meaning. Even though the parameters in model-based approaches could closely link with the physical characteristics, the extrication of these parameters is difficult especially for the electrochemical model where a series of reactions happens simultaneously. Furthermore, since the battery is a nonlinear system, the parameters extracted are often restricted to certain operating conditions and have limited scalability.

VI. Outlook

Although numerous efforts have been made on the fast-charging control and optimization, further improvements are desired in the following issues.

Multi-physics coupled model is preferred for comprehensively considering the internal mechanism during charging progress. With the help of a multi-physics coupled model, we could monitor the undesired safety-related reactions like lithium deposition [217-221]. Generally, the battery model will become more complicated while describing more physical phenomena. As a result, developing a simplified multi-physics coupled model which can improve the computation efficiency without sacrificing accuracy is a constant pursuit. Chu et al. propose a reduced-order electrochemical model to reduce the computational complexity [219]. A decomposed electrode model based on the equivalent circuit model is used to prevent lithium deposition during fast charging [220]. A real-time anode potential estimation is achieved by the novel model with low complexity. The transmission line model can be considered as a kind of physics-based equivalent circuit model that can describe the charge transfer and ion diffusion process [221].

Multi-physics constrained charging control strategy can be developed prosperously under the improvement of the multi-physics coupled model. For instance, coupled with an anode potential model, the lithium deposition reaction can be limited during fast charging [220]. In addition, online detection methods can provide another way to constrain crucial side reactions. A new method of lithium deposition onset detection during fast charging is proposed using operando electrochemical impedance spectroscopy [222]. The online analysis of the voltage relaxation profile also can be used to detect the onset of lithium deposition [223]. This detection method is used for the development of plating-free charging strategies at low temperatures. More online detection method is preferred to realize the multi-physics constrained control strategy.

With the development of machine learning, data-driven machine learning is widely used in the field including modeling, state estimation, and optimization. Furthermore, machine learning can also be used for optimal charging. A closed-loop optimization of fast charging protocols is proposed using machine learning [210]. In this approach, high cycle life charging protocols are identified by predicting the final cycle life using data from the first few cycles. A DRL-based optimizer is proposed to provide a LIB fast charging solution [212]. In addition, modeling and state estimation based on machine learning can improve the optimal charging strategies. For instance, purely physics-based models and purely data-driven models have advantages and limitations of their own and combining physics-based and machine learning models can leverage their respective strengths [224, 225]. Several possible integration architectures are outlined in [226] for physics-based and machine learning models.

VII. Conclusion

The long charging time hampers the broad acceptance of electric vehicles. The optimization of the charging process has been studied vastly over the last decade. This paper aims to promote the optimization approaches by a comprehensive review. At first, this paper explains the principles of lithium-ion battery charging including battery operation mechanism, simulation models, and aging mechanisms. This lays a solid foundation and also answers the question of why charging optimization is essential. Then, the structure of charging optimization approaches is formed which to the authors' knowledge is the first of its kind. According to this structure, researches is clustered as open- and closed-loop optimization approaches. Some major conclusions are summarized as follows.

The open-loop charging optimization is characterized by profile-based approaches, like boost charging, multi-stage constant current charging, pulse/sinusoidal wave charging. The multi-stage constant current charging shows to be promising concerning the presented testing results. However, only part of the critical objectives like charging time reduction and battery temperature regulation are focused on in most of the works. Extra concerns such as charge efficiency, safety degradation, and aging should be taken into account in the future.

The closed-loop optimizations are categorized as model-based approaches and data-driven approaches. The model-based closed-loop charging optimization approaches are promising considering the merits of environmental adaptive property. However, high-fidelity modeling is the prerequisite. Electrical equivalent circuit models coupled with electro-thermal models can be a preferable solution even though they can only reflect very limited physical characteristics. Electrochemical model-based approaches remedy this deficiency, but are generally computation-intensive and not suitable for real-time applications. Closed-loop charging approaches with awareness of multiple mechanisms, especially for the aging, and feasible for real-time application is critical but still an open issue.

Data-driven approaches are emerging due to the blooming of data science. In these approaches, the battery is treated as a black box, which leaves out the complexity caused by the models and could be applied online. The main controversial point is the application of pre-tests. Even though there is limited research about data-driven approaches so far, the data-driven approaches can appeal for future deployment concerning the unique advantages over model-based ones.

In conclusion, the principal knowledge of multi-physics in lithium-ion batteries is a prerequisite for model-based charging optimization approaches. To this point, the coupling of models describing multiple processes is preferable considering the intrinsic multi-constrained property of charging optimization problems. Besides, since aging characteristics also vary with operating conditions and the type of the battery, enhanced electrochemical models which could reflect aging characteristics are of paramount importance. Furthermore, as the electrochemical models are generally computational intensive, there is currently only limited research that considers the influence of aging for online/real-time applications. Data-driven approaches could be applied for online/ real-time applications. However, indicators in data-driven approaches do not have physical meanings, thus it is challenging for interpretation. In the future, the exploration of control-oriented, multi-physics aware yet computationally affordable models are the key task.

VIII. GLOSSARY

Abbreviation	Explanation	Abbreviation	Explanation
AM	Aging Mechanism	LIB	Lithium-ion Battery
BEV	Battery Electric Vehicle	MCC	Multi-stage Constant Current charging
BiR	Built-in Resistance	mOBGG	multi-Objective Biogeography-based Optimization
CC-CV	Constant Current-Constant Voltage	MPC	Model Predictive Control
CCS	Combined Charging System	NCA	Lithium Nickel Cobalt Aluminum Oxide
CEI	Cathode-Electrolyte Interphase	NMC	Lithium Nickel Manganese Cobalt Oxide
ChgOp	Charging Optimization	P2D	Pseudo-two-Dimensional
CP-CV	Constant Power-Constant Voltage	PSO	Particle Swarm Optimizer
CT-CV	Constant Temperature-Constant Voltage	PW	Pulse Wave
DMC	Dimethyl Carbonate	QDMC	Quadratic Dynamic Matrix Control
DRL	Deep Reinforcement Learning	RL	Reinforcement Learning
EC	Ethylene Carbonate	ROM	reduced-order electrochemical model
EcM	Electrochemical Model	SEI	Solid Electrolyte Interphase
ECM	Electrical Equivalent Circuit Model	SoC	State of Charge
XFC	Extreme Fast Charging	SoH	State of Health
EtM	Electro-thermal Model	SPM	Single-Particle Model
EV	Electric Vehicles	SW	Sinusoidal Wave
LCO	Lithium Cobalt Oxide	UVP	Universal Voltage Control Protocol
LFP	Lithium Iron Phosphate	VCD	Varying Current Decay

REFERENCES

[1] H. Tu, H. Feng, S. Srdic, and S. Lukic, "Extreme Fast Charging of Electric Vehicles: A Technology Overview," *IEEE Transactions on Transportation Electrification,* vol. 5, pp. 861-878, 2019.

[2] T. R. Tanim, E. J. Dufek, M. Evans, C. Dickerson, A. N. Jansen, B. J. Polzin*, et al.*, "Extreme Fast Charge Challenges for Lithium-Ion Battery: Variability and Positive Electrode Issues," *Journal of The Electrochemical Society,* vol. 166, pp. A1926-A1938, 2019.

[3] M. R. Khalid, M. S. Alam, A. Sarwar, and M. S. Jamil Asghar, "A Comprehensive review on electric vehicles charging infrastructures and their impacts on power-quality of the utility grid," *eTransportation,* vol. 1, p. 100006, 2019/08/01/ 2019.

[4] D. E. S. Demirocak, S.S.; Stefanakos, E.K., "A Review on Nanocomposite Materials for Rechargeable Li-ion Batteries," *Applied sciences,* vol. 7, 2017.

[5] U. Consortium. (1996). *Electric Vehicle Battery Test Procedures Manual*.

[6] C. Pillot, "The worldwide battery market 2012-2025," presented at the BATTERIES 2013, Nice, FRANCE, 2013.

[7] J. Warner, "Chapter 2 - History of Vehicle Electrification," in *The Handbook of Lithium-Ion Battery Pack Design*, J. Warner, Ed., ed Amsterdam: Elsevier, 2015, pp. 9-21.

[8] B. University. (2018). *BU-409: Charging Lithium-ion*.

[9] P. H. L. Notten, J. H. G. O. h. Veld, and J. R. G. v. Beek, "Boostcharging Li-ion batteries: A challenging new charging concept," *Journal of Power Sources,* vol. 145, pp. 89-94, 2005/07/04/ 2005.

[10] Y. Lee and S. Park, "Rapid charging strategy in the constant voltage mode for a high power Li-Ion battery," in *2013 IEEE Energy Conversion Congress and Exposition*, 2013, pp. 4725-4731.

[11] C. Wenlong, Y. Yao, G.-L. Zhu, Y. Chong, L.-L. Jiang, C. He*, et al.*, "A review on energy chemistry of fast-charging anodes," *Chemical Society Reviews,* vol. 49, 06/01 2020.

[12] S. E. D. Corporation and D. S. B. G. S. Corporation. (2014). *Sony FTC1 18650 Battery, 1100mAh, 20A, 3.2V, Grade A Lithium-ion*. Available: https://voltaplex.com/sony-ftc1-18650-battery-us18650ftc1

[13] M. M. Hoque, M. A. Hannan, A. Mohamed, and A. Ayob, "Battery charge equalization controller in electric vehicle applications: A review," *Renewable & Sustainable Energy Reviews,* vol. 75, pp. 1363-1385, Aug 2017.

[14] Y. Liu, Y. Zhu, and Y. Cui, "Challenges and opportunities towards fast-charging battery materials," *Nature Energy,* vol. 4, pp. 540-550, 2019/07/01 2019.

[15] G.-L. Zhu, C.-Z. Zhao, J.-Q. Huang, C. He, J. Zhang, S. Chen*, et al.*, "Fast Charging Lithium Batteries: Recent Progress and Future Prospects," *Small,* vol. 15, p. 1805389, 2019/04/01 2019.

[16] M. Parchomiuk, A. Moradewicz, and H. Gawinski, *An Overview of Electric Vehicles Fast Charging Infrastructure*, 2019.

[17] D. Sauer and F. Ringbeck, *Battery-electric vehicles at the eve to make the major breakthrough - Upcoming challenges on materials, batteries, and the energy system*, 2019.

[18] B. University. (2019). *BU-1003: Electric Vehicle (EV)*.

[19] W. Khan, A. Ahmad, F. Ahmad, and M. S. Alam, "A Comprehensive Review of Fast Charging Infrastructure for Electric Vehicles," *Smart Science,* vol. 6, pp. 256-270, 2018 2018.

[20] S. F. Till Gnann, Niklas Jakobsson, Patrick Plötz, Frances Sprei, Anders Bennehag, "Fast charging infrastructure for electric vehicles: Today's situation and future needs," *Transportation Research Part D,* pp. 314-329, 2018.

[21] D. Meyer and W. Jiankang, "Integrating ultra-fast charging stations within the power grids of smart cities: a review," *IET Smart Grid,* vol. 1, pp. 3-10, April 2018.

[22] B. Group. (2018). *Research project "FastCharge": ultra-fast charging technology ready for the electrically powered vehicles of the future.* Available:

[23] V. S. P. a. S. Gillard. (2019). *X-CEL: eXtreme Fast Charge Cell Evaluation of Lithium-ion Batteries*.

[24] A. Tomaszewska, Z. Chu, X. Feng, S. O'Kane, X. Liu, J. Chen*, et al.*, "Lithium-ion battery fast charging: A review," *eTransportation,* vol. 1, p. 100011, 2019/08/01/ 2019.

[25] W. Xie, X. Liu, R. He, Y. Li, X. Gao, X. Li*, et al.*, "Challenges and opportunities toward fast-charging of lithium-ion batteries," *Journal of Energy Storage,* vol. 32, p. 101837, 2020/12/01/ 2020.

[26] M. Ahmadi, N. Mithulananthan, and R. Sharma, *A review on topologies for fast charging stations for electric vehicles*, 2016.

[27] M. A. H. Rafi and J. Bauman, "A Comprehensive Review of DC Fast-Charging Stations With Energy Storage: Architectures, Power Converters, and Analysis," *IEEE Transactions on Transportation Electrification,* vol. 7, pp. 345-368, 2021.

[28] D. Dobrzanski, "Overview and characteristics of the EV fast charging connector systems," *Maszyny Elektryczne - Zeszyty Problemowe,* vol. 115, pp. 91-6, 2017 2017.

[29] A. Ahmad, M. S. Alam, and R. Chabaan, "A Comprehensive Review of Wireless Charging Technologies for Electric Vehicles," *IEEE Transactions on Transportation Electrification,* vol. 4, pp. 38-63, 2018.

[30] K. Mude and K. Aditya, "Comprehensive review and analysis of two-element resonant compensation topologies for wireless inductive power transfer systems," *Chinese Journal of Electrical Engineering,* vol. 5, pp. 14-31, 2019.

[31] Y. Gao, X. Zhang, Q. Cheng, B. Guo, and J. Yang, "Classification and Review of the Charging Strategies for Commercial Lithium-Ion Batteries," *IEEE Access,* vol. 7, pp. 43511-43524, 2019.

[32] Q. Lin, J. Wang, R. Xiong, W. Shen, and H. He, "Towards a smarter battery management system: A critical review on optimal charging methods of lithium ion batteries," *Energy,* vol. 183, pp. 220-234, 2019/09/15/ 2019.

[33] A. Yoshino, "The Birth of the Lithium-Ion Battery," *Angewandte Chemie International Edition,* vol. 51, pp. 5798-5800, 2012/06/11 2012.

[34] C. Yan, R. Xu, Y. Xiao, J.-F. Ding, L. Xu, B.-Q. Li*, et al.*, "Toward Critical Electrode/Electrolyte Interfaces in Rechargeable Batteries," *Advanced Functional Materials,* vol. 30, p. 1909887, 2020/06/01 2020.

[35] T. M. Gür, "Review of electrical energy storage technologies, materials and systems: challenges and prospects for large-scale grid storage," *Energy & Environmental Science,* vol. 11, pp. 2696-2767, 2018.

[36] A. Ramar and F.-M. Wang, "Chapter 15 - Emerging anode and cathode functional materials for lithium-ion batteries," in *Nanostructured, Functional, and Flexible Materials for Energy Conversion and Storage Systems*, A. Pandikumar and P. Rameshkumar, Eds., ed: Elsevier, 2020, pp. 465-491.

[37] N. Nitta, F. Wu, J. T. Lee, and G. Yushin, "Li-ion battery materials: present and future," *Materials Today,* vol. 18, pp. 252-264, 2015/06/01/ 2015.

[38] Y. Liu, G. Zhou, K. Liu, and Y. Cui, "Design of Complex Nanomaterials for Energy Storage: Past Success and Future Opportunity," *Acc. Chem. Res.,* vol. 50, pp. 2895-2905, // 2017.

[39] R. Schmuch, R. Wagner, G. Horpel, T. Placke, and M. Winter, "Performance and cost of materials for lithium-based rechargeable automotive batteries," *Nature Energy,* vol. 3, pp. 267-278, Apr 2018.

[40] R. Yazami, "Surface chemistry and lithium storage capability of the graphite–lithium electrode," *Electrochimica Acta,* vol. 45, pp. 87-97, 1999/09/30/ 1999.

[41] P. Arora and Z. Zhang, "Battery Separators," *Chemical Reviews,* vol. 104, pp. 4419-4462, 2004/10/01 2004.

[42] M. Pagliaro and F. Meneguzzo, "The driving power of the electron," *Journal of Physics: Energy,* vol. 1, p. 011001, 11/20 2018.

[43] A. K. Padhi, "Phospho-olivines as Positive-Electrode Materials for Rechargeable Lithium Batteries," *Journal of The Electrochemical Society,* vol. 144, p. 1188, 1997.

[44] O. Toprakci, H. A. K. Toprakci, L. W. Ji, and X. W. Zhang, "Fabrication and Electrochemical Characteristics of LiFePO4 Powders for Lithium-Ion Batteries," *Kona Powder and Particle Journal,* pp. 50-73, 2010.

[45] S.-Y. Chung, J. T. Bloking, and Y.-M. Chiang, "Electronically conductive phospho-olivines as lithium storage electrodes," *Nature Materials,* vol. 1, pp. 123-128, 2002/10/01 2002.

[46] J. Wilhelm, S. Seidlmayer, P. Keil, J. Schuster, A. Kriele, R. Gilles*, et al.*, "Cycling capacity recovery effect: A coulombic efficiency and post-mortem study," *Journal of Power Sources,* vol. 365, pp. 327-338, 2017/10/15/ 2017.

[47] R. Fong, U. von Sacken, and J. R. Dahn, "Studies of Lithium Intercalation into Carbons Using Nonaqueous Electrochemical Cells," *Journal of The Electrochemical Society,* vol. 137, pp. 2009-2013, 1990/07/01 1990.

[48] M. A. Roscher, J. Vetter, and D. U. Sauer, "Characterisation of charge and discharge behaviour of lithium ion batteries with olivine based cathode active material," *Journal of Power Sources,* vol. 191, pp. 582-590, 2009/06/15/ 2009.

[49] D. Anseán, M. González, J. C. Viera, V. M. García, C. Blanco, and M. Valledor, "Fast charging technique for high power lithium iron phosphate batteries: A cycle life analysis," *Journal of Power Sources,* vol. 239, pp. 9-15, 2013/10/01/ 2013.

[50] B. Y. L. Zhen Guo, Xinping Qiu, Lanlan Gao, Changshui Zhang, "Optimal charging method for lithium ion batteries using a universal voltage protocol accommodating aging," *Journal of Power Sources,* vol. 274, p. 957e964, 2015.

[51] S. S. Zhang, "The effect of the charging protocol on the cycle life of a Li-ion battery," *Journal of power sources,* vol. 161, pp. 1385-1391, 2006.

[52] I. H. Cho, P. Y. Lee, and J. H. Kim, "Analysis of the effect of the variable charging current control method on cycle life of Li-ion batteries," *Energies,* vol. 14, 2019.

[53] D. Anseán, M. Dubarry, A. Devie, B. Y. Liaw, V. M. García, J. C. Viera*, et al.*, "Fast charging technique for high power LiFePO4 batteries: A mechanistic analysis of aging," *Journal of Power Sources,* vol. 321, pp. 201-209, 2016/07/30/ 2016.

[54] F. Grimsmann, T. Gerbert, F. Brauchle, A. Gruhle, J. Parisi, and M. Knipper, "Determining the maximum charging currents of lithium-ion cells for small charge quantities," *Journal of Power Sources,* vol. 365, pp. 12-16, 2017.

[55] M. Doyle, T. F. Fuller, and J. Newman, "Modeling of Galvanostatic Charge and Discharge of the Lithium/Polymer/Insertion Cell," *Journal of The Electrochemical Society,* vol. 140, pp. 1526-1533, June 1, 1993 1993.

[56] M. Torchio, N. A. Wolff, D. M. Raimondo, L. Magni, U. Krewer, R. B. Gopaluni*, et al.*, "Real-time model predictive control for the optimal charging of a lithium-ion battery," in *2015 American Control Conference (ACC)*, 2015, pp. 4536-4541.

[57] C. F. Zou, X. S. Hu, Z. B. Wei, T. Wik, and B. Egardt, "Electrochemical Estimation and Control for Lithium-Ion Battery Health-Aware Fast Charging," *Ieee Transactions on Industrial Electronics,* vol. 65, pp. 6635-6645, Aug 2018.

[58] R. Methekar, "SOC estimation with thermal and charging rate consideration using dual filter approach for lithium-ion battery," *Journal of Renewable and Sustainable Energy,* vol. 10, p. 12, Nov 2018.

[59] D. Zhang, B. N. Popov, and R. E. White, "Modeling Lithium Intercalation of a Single Spinel Particle under Potentiodynamic Control," *Journal of The Electrochemical Society,* vol. 147, p. 831, 2000.

[60] R. Klein, N. A. Chaturvedi, J. Christensen, J. Ahmed, R. Findeisen, and A. Kojic, "Optimal charging strategies in lithium-ion battery," in *Proceedings of the 2011 American Control Conference*, 2011, pp. 382-387.

[61] Y. Li, Z. Wei, B. Xiong, and D. M. Vilathgamuwa, "Adaptive ensemble-based electrochemical-thermal-degradation state estimation of lithium-ion batteries," *IEEE Transactions on Industrial Electronics,* 2021.

[62] M. Song and S.-Y. Choe, "Fast and safe charging method suppressing side reaction and lithium deposition reaction in lithium ion battery," *Journal of Power Sources,* vol. 436, p. 226835, 2019.

[63] X. Hu, S. Li, and H. Peng, "A comparative study of equivalent circuit models for Li-ion batteries," *Journal of Power Sources,* vol. 198, pp. 359-367, 2012/01/15/ 2012.

[64] Z. Wei, C. Zou, F. Leng, B. H. Soong, and K.-J. Tseng, "Online model identification and state-of-charge estimate for lithium-ion battery with a recursive total least squares-based observer," *IEEE Transactions on Industrial Electronics,* vol. 65, pp. 1336-1346, 2017.

[65] Z. Wei, H. He, J. Pou, K. L. Tsui, Z. Quan, and Y. Li, "Signal-Disturbance Interfacing Elimination for Unbiased Model Parameter Identification of Lithium-Ion Battery," *IEEE Transactions on Industrial Informatics,* pp. 1-1, 2020.

[66] G. L. Plett, "Extended Kalman filtering for battery management systems of LiPB-based HEV battery packs: Part 3. State and parameter estimation," *Journal of Power Sources,* vol. 134, pp. 277-292, 8/12/ 2004.

[67] Z. Wei, J. Hu, Y. Li, H. He, W. Li, and D. U. Sauer, "Hierarchical soft measurement of load current and state of charge for future smart lithium-ion batteries," *Applied Energy,* vol. 307, p. 118246, 2022.

[68] Z. G. Wei, J. Hu, H. He, Y. Li, and B. Xiong, "Load Current and State of Charge Co-Estimation for Current Sensor-Free Lithium-ion Battery," *IEEE Transactions on Power Electronics,* 2021.

[69] Z. Wei, J. Zhao, R. Xiong, G. Dong, J. Pou, and K. J. Tseng, "Online Estimation of Power Capacity With Noise Effect Attenuation for Lithium-Ion Battery," *IEEE Transactions on Industrial Electronics,* vol. 66, pp. 5724-5735, 2019.

[70] X. Hu, Y. Zheng, X. Lin, and Y. Xie, "Optimal Multistage Charging of NCA/Graphite Lithium-Ion Batteries Based on Electrothermal-Aging Dynamics," *IEEE Transactions on Transportation Electrification,* vol. 6, pp. 427-438, 2020.

[71] L. Patnaik, A. Praneeth, and S. S. Williamson, "A Closed-Loop Constant-Temperature Constant-Voltage Charging Technique to Reduce Charge Time of Lithium-Ion Batteries," *Ieee Transactions on Industrial Electronics,* vol. 66, pp. 1059-1067, Feb 2019.

[72] K. Liu, C. Zou, K. Li, and T. Wik, "Charging Pattern Optimization for Lithium-Ion Batteries With an Electrothermal-Aging Model," *IEEE Transactions on Industrial Informatics,* vol. 14, pp. 5463-5474, 2018.

[73] A. B. Khan and W. Choi, "Optimal Charge Pattern for the High-Performance Multistage Constant Current Charge Method for the Li-Ion Batteries," *IEEE Transactions on Energy Conversion,* vol. 33, pp. 1132-1140, 2018.

[74] N. Tian, H. Fang, and Y. Wang, "Real-Time Optimal Lithium-Ion Battery Charging Based on Explicit Model Predictive Control," *IEEE Transactions on Industrial Informatics,* pp. 1-1, 2020.

[75] Y. Luo, Y. Liu, and S. Wang, "Search for an optimal multistage charging pattern for lithium-ion batteries using the Taguchi approach," in *TENCON 2009 - 2009 IEEE Region 10 Conference*, 2009, pp. 1-5.

[76] H. E. Perez, X. Hu, S. Dey, and S. J. Moura, "Optimal Charging of Li-Ion Batteries With Coupled Electro-Thermal-Aging Dynamics," *IEEE Transactions on Vehicular Technology,* vol. 66, pp. 7761-7770, 2017.

[77] T. Wang, C. Li, L. Chang, B. Duan, and C. Zhang, "Thermal behavior analysis of Pouch Lithium ion Battery using distributed electro-thermal model," in *2019 3rd Conference on Vehicle Control and Intelligence (CVCI)*, 2019, pp. 1-5.

[78] Y. Tang, L. Wu, W. Wei, D. Wen, Q. Guo, W. Liang*, et al.*, "Study of the thermal properties during the cyclic process of lithium ion power batteries using the electrochemical-thermal coupling model," *Applied Thermal Engineering,* vol. 137, pp. 11-22, 2018.

[79] M. Ghalkhani, F. Bahiraei, G.-A. Nazri, and M. Saif, "Electrochemical–thermal model of pouch-type lithium-ion batteries," *Electrochimica Acta,* vol. 247, pp. 569-587, 2017.

[80] Y. Xie, W. Li, X. Hu, C. Zou, F. Feng, and X. Tang, "Novel mesoscale electrothermal modeling for lithium-ion batteries," *IEEE Transactions on Power Electronics,* vol. 35, pp. 2595-2614, 2019.

[81] Y. Kim, S. Mohan, J. B. Siegel, A. G. Stefanopoulou, and Y. Ding, "The estimation of temperature distribution in cylindrical battery cells under unknown cooling conditions," *IEEE Transactions on Control Systems Technology,* vol. 22, pp. 2277-2286, 2014.

[82] G. Chen, Z. Liu, H. Su, and W. Zhuang, "Electrochemical-distributed thermal coupled model-based state of charge estimation for cylindrical lithium-ion batteries," *Control Engineering Practice,* vol. 109, p. 104734, 2021.

[83] M. Broussely, S. Herreyre, P. Biensan, P. Kasztejna, K. Nechev, and R. J. Staniewicz, "Aging mechanism in Li ion cells and calendar life predictions," *J. Power Sources,* vol. 97-98, pp. 13-21, // 2001.

[84] M. Jafari, K. Khan, and L. Gauchia, "Deterministic models of Li-ion battery aging: It is a matter of scale," *Journal of Energy Storage,* vol. 20, pp. 67-77, 2018/12/01/ 2018.

[85] M. Lucu, E. Martinez-Laserna, I. Gandiaga, and H. Camblong, "A critical review on self-adaptive Li-ion battery ageing models," *Journal of Power Sources,* vol. 401, pp. 85-101, 2018/10/15/ 2018.

[86] A. Barré, B. Deguilhem, S. GROLLEAU, M. Gérard, F. Suard, and D. Riu, "A review on lithium-ion battery ageing mechanisms and estimations for automotive applications," *Journal of Power Sources,* vol. 241, pp. 680 - 689, 2013-11 2013.

[87] M. Ecker, N. Nieto, S. Käbitz, J. Schmalstieg, H. Blanke, A. Warnecke*, et al.*, "Calendar and cycle life study of Li(NiMnCo)O2-based 18650 lithium-ion batteries," *Journal of Power Sources,* vol. 248, pp. 839-851, 2014/02/15/ 2014.

[88] I. Bloom, B. W. Cole, J. J. Sohn, S. A. Jones, E. G. Polzin, V. S. Battaglia*, et al.*, "An accelerated calendar and cycle life study of Li-ion cells," *Journal of Power Sources,* vol. 101, pp. 238-247, 2001/10/15/ 2001.

[89] M. Ecker, J. B. Gerschler, J. Vogel, S. Käbitz, F. Hust, P. Dechent*, et al.*, "Development of a lifetime prediction model for lithium-ion batteries based on extended accelerated aging test data," *Journal of Power Sources,* vol. 215, pp. 248-257, 2012/10/01/ 2012.

[90] M. Schimpe, M. E. von Kuepach, M. Naumann, H. C. Hesse, K. Smith, and A. Jossen, "Comprehensive Modeling of Temperature-Dependent Degradation Mechanisms in Lithium Iron Phosphate Batteries," *Journal of The Electrochemical Society,* vol. 165, pp. A181-A193, 2018.

[91] J. Wang, P. Liu, J. Hicks-Garner, E. Sherman, S. Soukiazian, M. Verbrugge*, et al.*, "Cycle-life model for graphite-LiFePO4 cells," *Journal of Power Sources,* vol. 196, pp. 3942-3948, 2011/04/15/ 2011.

[92] J. Z. Shen and T. Kosmač, "Chapter 1 - Introduction," in *Advanced Ceramics for Dentistry*, J. Z. Shen and T. Kosmač, Eds., ed Oxford: Butterworth-Heinemann, 2014, pp. 1-4.

[93] Y. Gao, J. Jiang, C. Zhang, W. Zhang, Z. Ma, and Y. Jiang, "Lithium-ion battery aging mechanisms and life model under different charging stresses," *J. Power Sources,* vol. 356, pp. 103-114, // 2017.

[94] G. Suri and S. Onori, "A control-oriented cycle-life model for hybrid electric vehicle lithium-ion batteries," *Energy,* vol. 96, pp. 644-653, 2016/02/01/ 2016.

[95] A. Millner, "Modeling Lithium Ion battery degradation in electric vehicles," in *2010 IEEE Conference on Innovative Technologies for an Efficient and Reliable Electricity Supply*, 2010, pp. 349-356.

[96] Z. Li, L. Lu, M. Ouyang, and Y. Xiao, "Modeling the capacity degradation of LiFePO4/graphite batteries based on stress coupling analysis," *Journal of Power Sources,* vol. 196, pp. 9757-9766, 2011/11/15/ 2011.

[97] N. Omar, M. A. Monem, Y. Firouz, J. Salminen, J. Smekens, O. Hegazy*, et al.*, "Lithium iron phosphate based battery - Assessment of the aging parameters and development of cycle life model," *Applied Energy,* vol. 113, pp. 1575-1585, Jan 2014.

[98] A. Cordoba-Arenas, S. Onori, Y. Guezennec, and G. Rizzoni, "Capacity and power fade cycle-life model for plug-in hybrid electric vehicle lithium-ion battery cells containing blended spinel and layered-oxide positive electrodes," *Journal of Power Sources,* vol. 278, pp. 473-483, 2015/03/15/ 2015.

[99] P. Atkins and J. d. Paula, *Atkins' Physical Chemistry*, 8th ed. Oxford; New York: Oxford University Press, 2006.

[100] T. Waldmann, M. Kasper, and M. Wohlfahrt-Mehrens, "Optimization of Charging Strategy by Prevention of Lithium Deposition on Anodes in high-energy Lithium-ion Batteries – Electrochemical Experiments," *Electrochimica Acta,* vol. 178, pp. 525-532, 2015/10/01/ 2015.

[101] H. Ruan, H. He, Z. Wei, Z. Quan, and Y. Li, "State of health estimation of lithium-ion battery based on constant-voltage charging reconstruction," *IEEE Journal of Emerging and Selected Topics in Power Electronics,* 2021.

[102] J. Vetter, P. Novák, M. R. Wagner, C. Veit, K. C. Möller, J. O. Besenhard, *et al.*, "Ageing mechanisms in lithium-ion batteries," *Journal of Power Sources,* vol. 147, pp. 269-281, 2005/09/09/ 2005.

[103] C. Schlasza, P. Ostertag, D. Chrenko, R. Kriesten, and D. Bouquain, "Review on the aging mechanisms in Li-ion batteries for electric vehicles based on the FMEA method," in *2014 IEEE Transportation Electrification Conference and Expo (ITEC)*, 2014, pp. 1-6.

[104] C. R. Birkl, M. R. Roberts, E. McTurk, P. G. Bruce, and D. A. Howey, "Degradation diagnostics for lithium ion cells," *Journal of Power Sources,* vol. 341, pp. 373-386, Feb 2017.

[105] J. O. Besenhard, M. Winter, J. Yang, and W. Biberacher, "Filming mechanism of lithium-carbon anodes in organic and inorganic electrolytes," *Journal of Power Sources,* vol. 54, pp. 228-231, 1995/04/01/ 1995.

[106] D. Aurbach, "Review of selected electrode–solution interactions which determine the performance of Li and Li ion batteries," *Journal of Power Sources,* vol. 89, pp. 206-218, 2000/08/01/ 2000.

[107] A. Wang, S. Kadam, H. Li, S. Shi, and Y. Qi, "Review on modeling of the anode solid electrolyte interphase (SEI) for lithium-ion batteries," *npj Computational Materials,* vol. 4, p. 15, 2018/03/26 2018.

[108] X.-G. Yang and C.-Y. Wang, "Understanding the trilemma of fast charging, energy density and cycle life of lithium-ion batteries," *Journal of Power Sources,* vol. 402, pp. 489-498, 2018/10/31/ 2018.

[109] F. An, R. Zhang, Z. Wei, and P. Li, "Multi-stage constant-current charging protocol for a high-energy-density pouch cell based on a 622NCM/graphite system," *RSC Advances,* vol. 9, pp. 21498-21506, 01/01 2019.

[110] N. Legrand, B. Knosp, P. Desprez, F. Lapicque, and S. Raël, "Physical characterization of the charging process of a Li-ion battery and prediction of Li plating by electrochemical modelling," *Journal of Power Sources,* vol. 245, pp. 208-216, 2014/01/01/ 2014.

[111] T. Waldmann, B.-I. Hogg, and M. Wohlfahrt-Mehrens, "Li plating as unwanted side reaction in commercial Li-ion cells – A review," *Journal of Power Sources,* vol. 384, pp. 107-124, 2018/04/30/ 2018.

[112] C. von Lüders, V. Zinth, S. V. Erhard, P. J. Osswald, M. Hofmann, R. Gilles, *et al.*, "Lithium plating in lithium-ion batteries investigated by voltage relaxation and in situ neutron diffraction," *Journal of Power Sources,* vol. 342, pp. 17-23, 2017/02/28/ 2017.

[113] R. Florian, R. Christiane, F. Georg, and S. Dirk Uwe, "Identification of Lithium Plating in Lithium-Ion Batteries by Electrical and Optical Methods," *Journal of the Electrochemical Society,* 2020.

[114] Y. M. Liu, G. N. B, J. L. Esbenshade, and A. A. Gewirth, "Characterization of the Cathode Electrolyte Interface in Lithium Ion Batteries by Desorption Electrospray Ionization Mass Spectrometry," *Anal Chem,* vol. 88, pp. 7171-7, Jul 19 2016.

[115] M. Wohlfahrt-Mehrens, C. Vogler, and J. Garche, "Aging mechanisms of lithium cathode materials," *Journal of Power Sources,* vol. 127, pp. 58-64, 2004/03/10/ 2004.

[116] M. Winter, K. C. Moeller, and J. O. Besenhard, "Carbonaceous and Graphitic Anodes," in *Lithium Batteries: Science and Technology*, G.-A. Nazri and G. Pistoia, Eds., ed Boston, MA: Springer US, 2003, pp. 145-194.

[117] R. Deshpande, M. Verbrugge, Y.-T. Cheng, J. Wang, and P. Liu, "Battery Cycle Life Prediction with Coupled Chemical Degradation and Fatigue Mechanics," *Journal of The Electrochemical Society,* vol. 159, pp. A1730-A1738, 2012.

[118] M. Cuisinier, J.-F. Martin, N. Dupré, A. Yamada, R. Kanno, and D. Guyomard, "Moisture driven aging mechanism of LiFePO4 subjected to air exposure," *Electrochemistry Communications,* vol. 12, pp. 238-241, 2010/02/01/ 2010.

[119] Y. Wang, X. Guo, S. Greenbaum, J. Liu, and K. Amine, "Solid Electrolyte Interphase Formation on Lithium-Ion Electrodes: A [sup 7]Li Nuclear Magnetic Resonance Study," *Electrochemical and Solid-State Letters,* vol. 4, p. A68, 2001.

[120] J. Christensen and J. Newman, "Stress generation and fracture in lithium insertion materials," *Journal of Solid State Electrochemistry,* vol. 10, pp. 293-319, 2006/05/01 2006.

[121] D. Aurbach, E. Zinigrad, Y. Cohen, and H. Teller, "A short review of failure mechanisms of lithium metal and lithiated graphite anodes in liquid electrolyte solutions," *Solid State Ionics,* vol. 148, pp. 405-416, // 2002.

[122] J. Wandt, "Operando Characterization of Fundamental Reaction Mechanisms and Degradation Processes in Lithium-Ion and Lithium-Oxygen Batteries," 2017.

[123] N. Lebedeva, F. D. Persio, and L. Boon-Brett, "Lithium ion battery value chain and related opportunities for Europe," https://ec.europa.eu/jrc/sites/jrcsh/files/jrc105010_161214_li-ion_battery_value_chain_jrc105010.pdf2016.

[124] Q. Liu, S. Li, S. Wang, X. Zhang, S. Zhou, Y. Bai, *et al.*, "Kinetically Determined Phase Transition from Stage II (LiC12) to Stage I (LiC6) in a Graphite Anode for Li-Ion Batteries," *The Journal of Physical Chemistry Letters,* vol. 9, pp. 5567-5573, 2018/09/20 2018.

[125] T. Ohzuku, Y. Iwakoshi, and K. Sawai, "Formation of Lithium - Graphite Intercalation Compounds in Nonaqueous Electrolytes and Their Application as a Negative Electrode for a Lithium Ion (Shuttlecock) Cell," *Journal of The Electrochemical Society,* vol. 140, pp. 2490-2498, 1993/09/01 1993.

[126] S. S. Zhang, K. Xu, and T. R. Jow, "Study of the charging process of a LiCoO2-based Li-ion battery," *Journal of Power Sources,* vol. 160, pp. 1349-1354, 2006/10/06/ 2006.

[127] P. Keil and A. Jossen, "Charging protocols for lithium-ion batteries and their impact on cycle life—An experimental study with different 18650 high-power cells," *Journal of Energy Storage,* vol. 6, pp. 125-141, 2016/05/01/ 2016.

[128] J. Hu, H. He, Z. Wei, and Y. Li, "Disturbance-immune and aging-robust internal short circuit diagnostic for lithium-ion battery," *IEEE Transactions on Industrial Electronics,* 2021.

[129] T. R. Jow, S. A. Delp, J. L. Allen, J.-P. Jones, and M. C. Smart, "Factors Limiting Li+Charge Transfer Kinetics in Li-Ion Batteries," *Journal of The Electrochemical Society,* vol. 165, pp. A361-A367, 2018.

[130] C. Mao, R. E. Ruther, J. Li, Z. Du, and I. Belharouak, "Identifying the limiting electrode in lithium ion batteries for extreme fast charging," *Electrochemistry Communications,* vol. 97, pp. 37-41, 2018/12/01/ 2018.

[131] T. Waldmann, B.-I. Hogg, M. Kasper, S. Grolleau, C. G. Couceiro, K. Trad, *et al.*, "Interplay of Operational Parameters on Lithium Deposition in Lithium-Ion Cells: Systematic Measurements with Reconstructed 3-Electrode Pouch Full Cells," *Journal of The Electrochemical Society,* vol. 163, pp. A1232-A1238, 2016.

[132] J. Zhu, Z. Sun, X. Wei, and H. Dai, "Studies on the medium-frequency impedance arc for Lithium-ion batteries considering various alternating current amplitudes," *Journal of Applied Electrochemistry,* vol. 46, pp. 157-167, 2016/02/01 2016.

[133] T. R. Jow, M. B. Marx, and J. L. Allen, "Distinguishing Li+Charge Transfer Kinetics at NCA/Electrolyte and Graphite/Electrolyte Interfaces, and NCA/Electrolyte and LFP/Electrolyte Interfaces in Li-Ion Cells," *Journal of The Electrochemical Society,* vol. 159, pp. A604-A612, 2012.

[134] J.-P. Jones, M. C. Smart, F. C. Krause, B. V. Ratnakumar, and E. J. Brandon, "The Effect of Electrolyte Composition on Lithium Plating During Low Temperature Charging of Li-Ion Cells," *ECS Transactions,* vol. 75, pp. 1-11, 2017/01/05 2017.

[135] B.-I. Hogg, "In Operando Li+- Activity Measurements in Lithium Ion Batteries - a Method to Develop and Optimize Safe Operating Strategies Even at Unfavourable Conditions," *ECS Meeting Abstracts,* 2015.

[136] B. Lu, Y. Zhao, Y. Song, and J. Zhang, "Stress-limited fast charging methods with time-varying current in lithium-ion batteries," *Electrochimica Acta,* vol. 288, pp. 144-152, 2018.

[137] C. P. Zhang, J. C. Jiang, Y. Gao, W. G. Zhang, Q. J. Liu, and X. S. Hu, "Charging optimization in lithium-ion batteries based on temperature rise and charge time," *Applied Energy,* vol. 194, pp. 569-577, May 2017.

[138] S. Cho, I. Lee, J. Baek, and G. Moon, "Battery Impedance Analysis Considering DC Component in Sinusoidal Ripple-Current Charging," *IEEE Transactions on Industrial Electronics,* vol. 63, pp. 1561-1573, 2016.

[139] J. Huang, Z. Li, and J. Zhang, "Dynamic electrochemical impedance spectroscopy reconstructed from continuous impedance measurement of single frequency during charging/discharging," *Journal of Power Sources,* vol. 273, pp. 1098-1102, 2015/01/01/ 2015.

[140] F. B. Spingler, W. Wittmann, J. Sturm, B. Rieger, and A. Jossen, "Optimum fast charging of lithium-ion pouch cells based on local volume expansion criteria," *Journal of Power Sources,* vol. 393, pp. 152-160, 2018/07/31/ 2018.

[141] Y. Yin and S.-Y. Choe, "Actively temperature controlled health-aware fast charging method for lithium-ion battery using nonlinear model predictive control," *Applied Energy,* vol. 271, p. 115232, 2020/08/01/ 2020.

[142] K. V. Kordesch, "Charging method for batteries, using the resistance-free voltage as endpoint indication," *J. Electrochem. Soc.,* vol. 119, pp. 1053-5, // 1972.

[143] T. Huang, R. Peng, T. Tsai, K. Chen, and C. Wey, "Fast Charging and High Efficiency Switching-Based Charger With Continuous Built-In Resistance Detection and Automatic Energy Deliver Control for Portable Electronics," *IEEE Journal of Solid-State Circuits,* vol. 49, pp. 1580-1594, 2014.

[144] Z. Wei, S. Meng, B. Xiong, D. Ji, and K. J. Tseng, "Enhanced online model identification and state of charge estimation for lithium-ion battery with a FBCRLS based observer," *Applied Energy,* vol. 181, pp. 332-341, 2016/11/01/ 2016.

[145] Z. Wei, J. Zhao, D. Ji, and K. J. Tseng, "A multi-timescale estimator for battery state of charge and capacity dual estimation based on an online identified model," *Applied Energy,* vol. 204, pp. 1264-1274, 2017/10/15/ 2017.

[146] X. Bian, Z. Wei, J. He, F. Yan, and L. Liu, "A Two-Step Parameter Optimization Method for Low-Order Model-Based State-of-Charge Estimation," *IEEE Transactions on Transportation Electrification,* vol. 7, pp. 399-409, 2021.

[147] X. Hu, S. Li, H. Peng, and F. Sun, "Robustness analysis of State-of-Charge estimation methods for two types of Li-ion batteries," *Journal of Power Sources,* vol. 217, pp. 209-219, 2012/11/01/ 2012.

[148] S. J. Drake, M. Martin, D. A. Wetz, J. K. Ostanek, S. P. Miller, J. M. Heinzel*, et al.*, "Heat generation rate measurement in a Li-ion cell at large C-rates through temperature and heat flux measurements," *Journal of Power Sources,* vol. 285, pp. 266-273, 2015/07/01/ 2015.

[149] Z. Wei, J. Zhao, H. He, G. Ding, H. Cui, and L. Liu, "Future smart battery and management: Advanced sensing from external to embedded multi-dimensional measurement," *Journal of Power Sources,* vol. 489, p. 229462, 2021/03/31/ 2021.

[150] X. Lin, H. E. Perez, J. B. Siegel, A. G. Stefanopoulou, Y. Li, R. D. Anderson*, et al.*, "Online Parameterization of Lumped Thermal Dynamics in Cylindrical Lithium Ion Batteries for Core Temperature Estimation and Health Monitoring," *IEEE Transactions on Control Systems Technology,* vol. 21, pp. 1745-1755, 2013.

[151] X. Bian, Z. Wei, J. He, F. Yan, and L. Liu, "A Novel Model-based Voltage Construction Method for Robust State-of-health Estimation of Lithium-ion Batteries," *IEEE Transactions on Industrial Electronics,* pp. 1-1, 2020.

[152] J. He, Z. Wei, X. Bian, and F. Yan, "State-of-Health Estimation of Lithium-Ion Batteries Using Incremental Capacity Analysis Based on Voltage–Capacity Model," *IEEE Transactions on Transportation Electrification,* vol. 6, pp. 417-426, 2020.

[153] C. E. Aimo and P. A. Aguirre, "Lithium-ion whole-cell design and charging protocol optimization within safe operating conditions," *Journal of Energy Storage,* vol. 30, 2020.

[154] M. Berecibar, I. Gandiaga, I. Villarreal, N. Omar, J. Van Mierlo, and P. Van den Bossche, "Critical review of state of health estimation methods of Li-ion batteries for real applications," *Renewable and Sustainable Energy Reviews,* vol. 56, pp. 572-587, 2016/04/01/ 2016.

[155] Y. Li, K. Liu, A. M. Foley, A. Zülke, M. Berecibar, E. Nanini-Maury*, et al.*, "Data-driven health estimation and lifetime prediction of lithium-ion batteries: A review," *Renewable and Sustainable Energy Reviews,* vol. 113, p. 109254, 2019/10/01/ 2019.

[156] A. Guha and A. Patra, "State of Health Estimation of Lithium-Ion Batteries Using Capacity Fade and Internal Resistance Growth Models," *IEEE Transactions on Transportation Electrification,* vol. 4, pp. 135-146, 2018.

[157] P. Shen, M. G. Ouyang, L. G. Lu, J. Q. Li, and X. N. Feng, "The Co-estimation of State of Charge, State of Health, and State of Function for Lithium-Ion Batteries in Electric Vehicles," *Ieee Transactions on Vehicular Technology,* vol. 67, pp. 92-103, Jan 2018.

[158] A. Eddahech, O. Briat, N. Bertrand, J.-Y. Delétage, and J.-M. Vinassa, "Behavior and state-of-health monitoring of Li-ion batteries using impedance spectroscopy and recurrent neural networks," *International Journal of Electrical Power & Energy Systems,* vol. 42, pp. 487-494, 2012/11/01/ 2012.

[159] M. Gholizadeh and F. R. Salmasi, "Estimation of State of Charge, Unknown Nonlinearities, and State of Health of a Lithium-Ion Battery Based on a Comprehensive Unobservable Model," *IEEE Transactions on Industrial Electronics,* vol. 61, pp. 1335-1344, 2014.

[160] Y. Li, M. Abdel-Monem, R. Gopalakrishnan, M. Berecibar, E. Nanini-Maury, N. Omar*, et al.*, "A quick on-line state of health estimation method for Li-ion battery with incremental capacity curves processed by Gaussian filter," *Journal of Power Sources,* vol. 373, pp. 40-53, Jan 2018.

[161] C. Weng, Y. Cui, J. Sun, and H. Peng, "On-board state of health monitoring of lithium-ion batteries using incremental capacity analysis with support vector regression," *Journal of Power Sources,* vol. 235, pp. 36-44, 2013/08/01/ 2013.

[162] X. Wang, X. Wei, and H. Dai, "Estimation of state of health of lithium-ion batteries based on charge transfer resistance considering different temperature and state of charge," *Journal of Energy Storage,* vol. 21, pp. 618-631, 2019/02/01/ 2019.

[163] Y. Wang, G. Gao, X. Li, and Z. Chen, "A fractional-order model-based state estimation approach for lithium-ion battery and ultra-capacitor hybrid power source system considering load trajectory," *Journal of Power Sources,* vol. 449, p. 227543, 2020.

[164] B. Purushothaman and U. Landau, "Rapid Charging of Lithium-Ion Batteries Using Pulsed Currents," *Journal of The Electrochemical Society,* vol. 153, pp. A533-A542, 03/01 2006.

[165] D. W. Gaddes, "The Effects of Pulsed Charging on Lithium Ion Batteries," George W Woodruff School of Mechanical Engineering, 2016.

[166] Y. Liu, C. Hsieh, and Y. Luo, "Search for an Optimal Five-Step Charging Pattern for Li-Ion Batteries Using Consecutive Orthogonal Arrays," *IEEE Transactions on Energy Conversion,* vol. 26, pp. 654-661, 2011.

[167] F. R. Xue, Z. Ling, Y. B. Yang, and X. P. Miao, "Design and Implementation of Novel Smart Battery Management System for FPGA Based Portable Electronic Devices," *Energies,* vol. 10, p. 14, Mar 2017.

[168] A. B. Khan, P. Van-Long, N. Thanh-Tung, and C. Woojin, "Multistage constant-current charging method for Li-Ion batteries," in *2016 IEEE Transportation Electrification Conference and Expo, Asia-Pacific (ITEC Asia-Pacific)*, 2016, pp. 381-385.

[169] M. T. Abdel Monem, Khiem ; Omar, Noshin; Hegazy, Omar; Mantels, Bart; Van Den Bossche, Peter; Van Mierlo, Joeri., "A comparative study of different fast charging methodologies for lithium-ion batteries based on aging process.," presented at the the 28th International Electric Vehicle Symposium and Exhibition (EVS28), KINTEX, Korea, 2015.

[170] M. Abdel-Monem, K. Trad, N. Omar, O. Hegazy, P. Van den Bossche, and J. Van Mierlo, "Influence analysis of static and dynamic fast-charging current profiles on ageing performance of commercial lithium-ion batteries," *Energy,* vol. 120, pp. 179-191, 2017/02/01/ 2017.

[171] T. T. Vo, X. Chen, W. Shen, and A. Kapoor, "New charging strategy for lithium-ion batteries based on the integration of Taguchi method and state of charge estimation," *Journal of Power Sources,* vol. 273, pp. 413-422, 2015.

[172] F. An, R. Zhang, Z. Wei, and P. Li, "Multi-stage constant-current charging protocol for a high-energy-density pouch cell based on a 622NCM/graphite system," *RSC Advances,* vol. 9, pp. 21498-21506, 2019.

[173] Y. Liu and Y. Luo, "Search for an Optimal Rapid-Charging Pattern for Li-Ion Batteries Using the Taguchi Approach," *IEEE Transactions on Industrial Electronics,* vol. 57, pp. 3963-3971, 2010.

[174] J. M. Amanor-Boadu, A. Guiseppi-Elie, and E. Sánchez-Sinencio, "Search for Optimal Pulse Charging Parameters for Li-Ion Polymer Batteries Using Taguchi Orthogonal Arrays," *IEEE Transactions on Industrial Electronics,* vol. 65, pp. 8982-8992, 2018.

[175] L. T. Lam, H. Ozgun, L. M. D. Cranswick, and D. A. J. Rand, "Pulsed-current formation of tetrabasic lead sulfate in cured lead/acid battery plates," *Journal of Power Sources,* vol. 42, pp. 55-70, 1993/01/29/ 1993.

[176] H. Lv, X. Huang, and Y. Liu, "Analysis on pulse charging–discharging strategies for improving capacity retention rates of lithium-ion batteries," *Ionics,* vol. 26, pp. 1749-1770, 2020/04/01 2020.

[177] F. Savoye, P. Venet, S. Pelissier, M. Millet, and J. Groot, "Impact of periodic current pulses on Li-ion batteries lifetime in vehicular application," *International Journal of Electric and Hybrid Vehicles,* vol. 7, p. 323, 01/01 2015.

[178] P. E. de Jongh and P. H. L. Notten, "Effect of current pulses on lithium intercalation batteries," *Solid State Ionics,* vol. 148, pp. 259-268, 2002/06/02/ 2002.

[179] B. Kwak, M. Kim, and J. Kim, "Add-On Type Pulse Charger for Quick Charging Li-Ion Batteries," *Electronics,* vol. 9, p. 227, 2020.

[180] Y. Zhao, B. Lu, Y. Song, and J. Zhang, "A modified pulse charging method for lithium-ion batteries by considering stress evolution, charging time and capacity utilization," *Frontiers of Structural and Civil Engineering,* vol. 13, pp. 294-302, 2019/04/01 2018.

[181] B. Purushothaman, P. Jr, and U. Landau, "Reducing Mass-Transport Limitations by Application of Special Pulsed Current Modes," *Journal of The Electrochemical Society - J ELECTROCHEM SOC,* vol. 152, 01/01 2005.

[182] D. N. Wong, D. A. Wetz, A. M. Mansour, and J. M. Heinzel, "The influence of high C rate pulsed discharge on lithium-ion battery cell degradation," in *2015 IEEE Pulsed Power Conference (PPC)*, 2015, pp. 1-6.

[183] D. N. Wong, D. A. Wetz, J. M. Heinzel, and A. N. Mansour, "Characterizing rapid capacity fade and impedance evolution in high rate pulsed discharged lithium iron phosphate cells for complex, high power loads," *Journal of Power Sources,* vol. 328, pp. 81-90, 2016/10/01/ 2016.

[184] Z. Wang, Y. Wang, Y. Rong, Z. Li, and L. Fantao, "Study on the Optimal Charging Method for Lithium-Ion Batteries Used in Electric Vehicles," *Energy Procedia,* vol. 88, pp. 1013-1017, 2016/06/01/ 2016.

[185] J. M. Amanor-Boadu, A. Guiseppi-Elie, and E. Sanchez-Sinencio, "The Impact of Pulse Charging Parameters on the Life Cycle of Lithium-Ion Polymer Batteries," *Energies,* vol. 11, p. 2162, 08/18 2018.

[186] B. Arabsalmanabadi, N. Tashakor, A. Javadi, and K. Al-Haddad, "Charging Techniques in Lithium-Ion Battery Charger: Review and New Solution," in *IECON 2018 - 44th Annual Conference of the IEEE Industrial Electronics Society*, 2018, pp. 5731-5738.

[187] L. Chen, W. Shing-Lih, and C. Tsair-Rong, "Improving battery charging performance by using sinusoidal current charging with the minimum AC impedance frequency," in *2010 IEEE International Conference on Sustainable Energy Technologies (ICSET)*, 2010, pp. 1-4.

[188] L. Chen, S. Wu, D. Shieh, and T. Chen, "Sinusoidal-Ripple-Current Charging Strategy and Optimal Charging Frequency Study for Li-Ion Batteries," *IEEE Transactions on Industrial Electronics,* vol. 60, pp. 88-97, 2013.

[189] A. Bessman, R. Soares, S. Vadivelu, O. Wallmark, P. Svens, H. Ekström, *et al.*, "Challenging Sinusoidal Ripple-Current Charging of Lithium-Ion Batteries," *IEEE Transactions on Industrial Electronics,* vol. 65, pp. 4750-4757, 2018.

[190] H. Z. Z. Beh, G. A. Covic, and J. T. Boys, "Effects of pulse and DC charging on lithium iron phosphate (LiFePO4) batteries," in *2013 IEEE Energy Conversion Congress and Exposition*, 2013, pp. 315-320.

[191] P.-T. Chen, F.-H. Yang, Z.-T. Cao, J.-M. Jhang, H.-M. Gao, M.-H. Yang, *et al.*, "Reviving Aged Lithium-Ion Batteries and Prolonging their Cycle Life by Sinusoidal Waveform Charging Strategy," *Batteries & Supercaps,* vol. 2, pp. 673-677, 2019/08/01 2019.

[192] G. Sikha, P. Ramadass, B. S. Haran, R. E. White, and B. N. Popov, "Comparison of the capacity fade of Sony US 18650 cells charged with different protocols," *Journal of Power Sources,* vol. 122, pp. 67-76, 2003/07/15/ 2003.

[193] F. P. Savoye, P. Venet, M. Millet, and J. Groot, "Impact of Periodic Current Pulses on Li-Ion Battery Performance," *IEEE Transactions on Industrial Electronics,* vol. 59, pp. 3481 - 3488, 2012-09 2012.

[194] J. Jiang, C. Zhang, J. Wen, W. Zhang, and S. M. Sharkh, "An Optimal Charging Method for Li-Ion Batteries Using a Fuzzy-Control Approach Based on Polarization Properties," *IEEE Transactions on Vehicular Technology,* vol. 62, pp. 3000-3009, 2013.

[195] H. Fang, C. Depcik, and V. Lvovich, "Optimal pulse-modulated Lithium-ion battery charging: Algorithms and simulation," *Journal of Energy Storage,* vol. 15, pp. 359-367, 02/01 2018.

[196] L. Chen, "Design of Duty-Varied Voltage Pulse Charger for Improving Li-Ion Battery-Charging Response," *IEEE Transactions on Industrial Electronics,* vol. 56, pp. 480-487, 2009.

[197] L. Chen, "A Design of an Optimal Battery Pulse Charge System by Frequency-Varied Technique," *IEEE Transactions on Industrial Electronics,* vol. 54, pp. 398-405, 2007.

[198] M. D. C. Yin, J.; Park, D. Pe., "Pulse-Based Fast Battery IoT Charger Using Dynamic Frequency and Duty Control Techniques Based on Multi-Sensing of Polarization Curve," *Energies,* vol. 9, 2016.

[199] R. Peng, T. Tsai, K. Chen, Z. H. Tai, Y. H. Cheng, C. C. Tsai, *et al.*, "Switching-based charger with continuously built-in resistor detector (CBIRD) and analog multiplication-division unit (AMDU) for fast charging in Li-Ion battery," in *2013 Proceedings of the ESSCIRC (ESSCIRC)*, 2013, pp. 157-160.

[200] K. Chung, S. Hong, and O. Kwon, "A Fast and Compact Charger for an Li-Ion Battery Using Successive Built-In Resistance Detection," *IEEE Transactions on Circuits and Systems II: Express Briefs,* vol. 64, pp. 161-165, 2017.

[201] C. Lin, C. Hsieh, and K. Chen, "A Li-Ion Battery Charger With Smooth Control Circuit and Built-In Resistance Compensator for Achieving Stable and Fast Charging," *IEEE Transactions on Circuits and Systems I: Regular Papers,* vol. 57, pp. 506-517, 2010.

[202] M. H. Noh, P. X. Thivel, C. Lefrou, and Y. Bultel, "Fast-charging of lithium iron phosphate battery with ohmic-drop compensation method," *Journal of Energy Storage,* vol. 8, pp. 160-167, 11/01 2016.

[203] S. Pramanik and S. Anwar, "Electrochemical model based charge optimization for lithium-ion batteries," *Journal of Power Sources,* vol. 313, pp. 164-177, 2016/05/01/ 2016.

[204] X. Lin, X. Hao, Z. Liu, and W. Jia, "Health conscious fast charging of Li-ion batteries via a single particle model with aging mechanisms," *Journal of Power Sources,* vol. 400, pp. 305-316, 2018/10/01/ 2018.

[205] A. Aryanfar, Y. Ghamlouche, and W. Goddard, *Control of Dendrites in Rechargeable Batteries using Smart Charging*, 2020.

[206] A. Aryanfar, M. Hoffmann, and W. Goddard, *Finite Pulse Waves for Efficient Suppression of Evolving Mesoscale Dendrites in Rechargeable Batteries*, 2019.

[207] Z. Chu, X. Feng, L. Lu, L. Jianqiu, X. Han, and M. Ouyang, "Non-destructive fast charging algorithm of lithium-ion batteries based on the control-oriented electrochemical model," *Applied Energy,* 03/01 2017.

[208] K. Liu, Z. Wei, Z. Yang, and K. Li, "Mass load prediction for lithium-ion battery electrode clean production: A machine learning approach," *Journal of Cleaner Production,* vol. 289, p. 125159, 2021/03/20/ 2021.

[209] S. Wang and Y. Liu, "A PSO-Based Fuzzy-Controlled Searching for the Optimal Charge Pattern of Li-Ion Batteries," *IEEE Transactions on Industrial Electronics,* vol. 62, pp. 2983-2993, 2015.

[210] P. M. Attia, A. Grover, N. Jin, K. A. Severson, T. M. Markov, Y.-H. Liao, *et al.*, "Closed-loop optimization of fast-charging protocols for batteries with machine learning," *Nature,* vol. 578, pp. 397-402, 2020/02/01 2020.

[211] I. J. Fernández, C. F. Calvillo, A. Sánchez-Miralles, and J. Boal, "Capacity fade and aging models for electric batteries and optimal charging strategy for electric vehicles," *Energy,* vol. 60, pp. 35-43, 2013/10/01/ 2013.

[212] Z. Wei, Z. Quan, J. Wu, Y. Li, J. Pou, and H. Zhong, "Deep Deterministic Policy Gradient-DRL Enabled Multiphysics-Constrained Fast Charging of Lithium-Ion Battery," *IEEE Transactions on Industrial Electronics,* pp. 1-1, 2021.

[213] J. B. Minho Kim, Soohee Han. (2020, Optimal Charging Method for Effective Li-ion Battery Life Extension Based on Reinforcement Learning.

[214] S. Park, A. Pozzi, M. Whitmeyer, H. Perez, W. Joe, D. M. Raimondo*, et al.*, *Reinforcement Learning-based Fast Charging Control Strategy for Li-ion Batteries*, 2020.

[215] J. Wu, Z. Wei, K. Liu, Z. Quan, and Y. Li, "Battery-Involved Energy Management for Hybrid Electric Bus Based on Expert-Assistance Deep Deterministic Policy Gradient Algorithm," *IEEE Transactions on Vehicular Technology,* vol. 69, pp. 12786-12796, 2020.

[216] J. Wu, Z. Wei, W. Li, Y. Wang, Y. Li, and D. U. Sauer, "Battery Thermal- and Health-Constrained Energy Management for Hybrid Electric Bus Based on Soft Actor-Critic DRL Algorithm," *IEEE Transactions on Industrial Informatics,* vol. 17, pp. 3751-3761, 2021.

[217] C. Zou, X. Hu, Z. Wei, T. Wik, and B. Egardt, "Electrochemical Estimation and Control for Lithium-Ion Battery Health-Aware Fast Charging," *IEEE Transactions on Industrial Electronics,* vol. 65, pp. 6635-6645, 2018.

[218] Z. Chu, R. Jobman, A. Rodríguez, G. L. Plett, M. S. Trimboli, X. Feng*, et al.*, "A control-oriented electrochemical model for lithium-ion battery. Part II: Parameter identification based on reference electrode," *Journal of Energy Storage,* vol. 27, 2020.

[219] Z. Chu, G. L. Plett, M. S. Trimboli, and M. Ouyang, "A control-oriented electrochemical model for lithium-ion battery, Part I: Lumped-parameter reduced-order model with constant phase element," *Journal of Energy Storage,* vol. 25, 2019.

[220] Y. Lu, X. Han, Z. Chu, X. Feng, Y. Qin, M. Ouyang*, et al.*, "A decomposed electrode model for real-time anode potential observation of lithium-ion batteries," *Journal of Power Sources,* vol. 513, 2021.

[221] M. Hahn, A. Schiela, P. Mößle, F. Katzer, and M. A. Danzer, "Revealing inhomogeneities in electrode lithiation using a real-time discrete electro-chemical model," *Journal of Power Sources,* vol. 477, 2020.

[222] D. E. Brown, E. J. McShane, Z. M. Konz, K. B. Knudsen, and B. D. McCloskey, "Detecting onset of lithium plating during fast charging of Li-ion batteries using operando electrochemical impedance spectroscopy," *Cell Reports Physical Science,* vol. 2, 2021.

[223] U. R. Koleti, C. Zhang, R. Malik, T. Q. Dinh, and J. Marco, "The development of optimal charging strategies for lithium-ion batteries to prevent the onset of lithium plating at low ambient temperatures," *Journal of Energy Storage,* vol. 24, 2019.

[224] T. Xie and J. C. Grossman, "Crystal Graph Convolutional Neural Networks for an Accurate and Interpretable Prediction of Material Properties," *Phys Rev Lett,* vol. 120, p. 145301, Apr 6 2018.

[225] G. C. Y. Peng, M. Alber, A. B. Tepole, W. R. Cannon, S. De, S. Dura-Bernal*, et al.*, "Multiscale modeling meets machine learning: What can we learn?," *Arch Comput Methods Eng,* vol. 28, pp. 1017-1037, May 2021.

[226] M. Aykol, C. B. Gopal, A. Anapolsky, P. K. Herring, B. van Vlijmen, M. D. Berliner*, et al.*, "Perspective—Combining Physics and Machine Learning to Predict Battery Lifetime," *Journal of The Electrochemical Society,* vol. 168, 2021.

Cuili Chen (Member, IEEE) received the B.Sc. and M.Sc. degrees from the School of Electrical Engineering, Dalian University of Technology, Dalian, China, in 2012 and 2015, respectively, and the Ph.D. degree from the School of Engineering, Newcastle University, Newcastle upon Tyne, U.K., in 2019.

She is currently holds a post-doctoral position at the Technical University of Munich, Munich, Germany. Her research interests include Li-ion batteries, battery management system, reliability of power semiconductor devices, active power filter, and switching power supplies.

Zhongbao Wei (M'19–SM'21) received the B.Eng. and the M.Sc. degrees in instrumental science and technology from Beihang University, China, in 2010 and 2013, and the Ph.D. degree in power engineering from Nanyang Technological University, Singapore, in 2017.

He has been a research fellow with Energy Research Institute @ NTU, Nanyang Technological University from 2016 to 2018. He is currently a professor in vehicle engineering with the National Engineering Laboratory for Electric Vehicles, Beijing Institute of Technology, China. He has authored more than 80 peer-reviewed articles. His research interests include electrified transportation and battery management. He serves as Associate Editor for many international journals like IEEE Transactions on Industrial Electronics, IEEE Transactions on Intelligent Transportation Systems, and IET Intelligent Transport Systems.

Alois C. Knoll (Senior Member, IEEE) has been a Professor with the Faculty of Computer Science, Technical University of Munich, Munich, Germany, since 2001, where he is currently a German Computer Scientist. He teaches and conducts research in the fields of autonomous systems, robotics, and artificial intelligence. From 2007 to 2009, he was a member of the EU's highest advisory board for information technology ISTAG. He was involved in the development of the EU flagship projects and one of the authors of the report "European Challenges and Flagships 2020 and Beyond." In 2009, he co-founded "fortiss," the Munich Institute for Software and Systems, which, due to its success, has since been transformed into a state institute of the State of Bavaria. He coordinated the EU project ECHORD++, a major initiative to bring new robot technology to market maturity. Since 2013, he has been the Head of the sub-project "Neurorobotics" of the Human Brain Project. Since 2015, he has been the Director of software development, i.e., one of three scientific directors of the HBP. He was a fellow of the School of Engineering, The University of Tokyo, Tokyo, Japan, in 2010. Prof. Knoll is a member of the German Society of Informatics.